The Pennsylvania State University

The Graduate School

Intercollege Graduate Degree Program in Physiology

THE CHICKEN MODEL OF OVARIAN CANCER: A NOVEL TP53 MRNA VARIANT FOUND IN HEALTHY AND CANCEROUS TISSUE

A Thesis in

Physiology

by

Aaron William Montani

Submitted in Partial Fulfillment
of the Requirements
for the Degree of

Master of Science

December 2014

The thesis of Aaron William Montani was reviewed and approved* by the following:

Ramesh Ramachandran
Associate Professor of Molecular Endocrinology
Thesis Advisor

Joy Pate
Professor of Reproductive Physiology

Alan L. Johnson
Walther H. Ott Professor in Avian Biology

Donna Korzick
Associate Professor of Physiology and Kinesiology
Chair, Intercollege Graduate Degree Program in Physiology

*Signatures are on file in the Graduate School

ABSTRACT

Ovarian cancer (OC) is a disease encompassing the highest death rate of any cancer of the female reproductive tract. It is the fifth leading cause of cancer related death among women, after lung, breast, colon, and pancreatic cancer. Ovarian tumors are difficult to diagnose early due to their location deep within the pelvis and a lack of sensitive, specific diagnostic biochemical tests. Currently, there are no established animal models of spontaneously occurring OC. The laying hen model of ovarian carcinoma is gaining acceptance as a model of OC, due to spontaneous generation of ovarian tumors as well as the similarity to human OC progression. Gene mutations are known to be concurrent with human cancers, including OC. The TP53 gene is a tumor suppressing gene known to be mutated in over 60% of human cancers. Mutations in TP53 have been associated with OC in humans. Point mutations of the TP53 mRNA transcript have been detected in chicken OC. The objective of this study was to compare chicken TP53 mRNA transcript in chicken OC with that of age-matched and young controls, ascites-derived chicken ovarian cancer cell lines, liver, and adipose tissue. Total RNA was extracted from ovarian tissue, ascites-derived ovarian cancer cell lines, liver and adipose tissue. Total RNA was reverse-transcribed to cDNA and the TP53 gene amplified by polymerase chain reaction (PCR) using gene-specific primers. The resultant PCR products were gel-purified and sequenced. Point mutations were discovered within the mRNA transcript. Interestingly, a deletion of 216 nucleotides spanning part of the transactivation domain and the entire proline-rich region was detected in all ovarian tumor, as well as age-matched and young healthy controls, ascites-derived chicken ovarian cancer cell lines, liver and adipose tissue. The deletion may be the result of yet unknown alternative splicing events during the biosynthesis of TP53 mRNA. The deletions

characterized in this study share similarity to isoforms of TP53 overexpressed in human cancer. In summary, alternative splicing events may produce a shorter form of the TP53 mRNA transcript that may contribute to the development of OC in chickens.

TABLE OF CONTENTS

LIST OF FIGURES

LIST OF TABLES

ACKNOWLEDGEMENTS

I want to thank my adviser Dr. Ramesh Ramachandran, without whom I would not have been able to succeed as a graduate student. I would also like to thank Jill Hadley and Anupama Tiwari, who helped me with my project from start to finish and were the sources of always needed advice and humor. Additionally I would like to thank my parents William and Sylvia Montani, and my sister, Elise Montani, for their continued support through my time at Penn State. Thank you to all of my friends for the stress relief that is so important during graduate school. Finally, I would like to thank my wonderful girlfriend Kristin Beiswenger. I could not have made it through the simultaneous demands of thesis writing, medical school applications, teaching, and life without your love and support.

Chapter 1

OC Statistics and Risk Factors

OC (OC) is a highly malignant disease that affects more than 21,000 women in the United States each year[1]. In the United States, it is the leading cause of death among women after lung, breast, colon, and pancreatic cancer, and accounts for 5% of cancer related deaths and 3% of the total incidence of cancer in women[1]. This rate of death is higher than any other cancer of the female reproductive tract[1]. The overall five year survival rate of ovarian carcinomas is 44%[2] . Stages III and IV have a less than 30% five year survival rate[1]. Stages I and II have higher (>80%) five year survival rate, but early diagnosis is uncommon[1].

There are several risk factors associated with development of OC. The most significant risk factor is a family history of OC, which may or may not include gene mutations[3]. Typically, a family history of cancer, especially breast cancer, implies a high risk for OC[3]. While there are numerous gene mutations associated with OC, mutations in BRCA1/2 impose a high risk of developing the disease[3]. Hereditary nonpolyposis colorectal cancer syndrome, an autosomal dominant disorder characterized by faulty DNA mismatch repair, also raises the risk of hereditary OC[3]. Despite this, hereditary disease accounts for only 12 percent of ovarian carcinomas[3]. Typically, cancer of the ovary develops on average at 51 years which is also the average age of menopause[4]. Other risk factors that are associated with ovarian tumors are obesity, smoking, and a sedentary lifestyle[3]. Certain physiological states are also associated with OC. Androgen and gonadotropin hypersecretion is known to occur in concert with PCOS, and is

associated with an increased risk of OC[5]. Additionally, most cases of OC occur during menopause[5]. Gonadotropin receptors are located on the ovarian epithelium and early tumor cells[5]. Hypersecretion of gonadotropins occurs during menopause, which may contribute to the early stages of tumor growth[5]. However, there is uncertainty in implicating hypersecretion of gonadotropins as a cause[6]. Some cases of OC also occur in individuals with suppressed gonadotropin secretion[6].

There are several methods of reducing the incidence of OC. Pregnancy, breastfeeding, and oral contraceptive use are associated with a decreased risk of OC[4]. Adequate intake of vitamins C and E, mono- and polyunsaturated fatty acids, exercise, and a diet low in fat are associated with a decreased risk of OC[3].

Anatomy of Human Ovary and Metastasis Classification

In humans, the ovaries are located deep within the pelvis, suspended by the broad, mesovarium, and proper ovarian ligaments[7]. The ovary is enclosed in a layer of mesothelial cells, and is comprised of an outer cortex and inner medulla[7]. The medulla houses blood vessels and connective tissue, and the cortex contains developing follicles in their various stages[7]. The ovaries are the primary sex organs and the vagina, cervix, uterus and fallopian tubes are accessory organs[7]. During ovulation, the mature oocyte is released from the ovary as the follicle ruptures and is picked up by the fimbriae of the fallopian tube with the remaining cells in the follicular cavity forming the corpus luteum[7].

Ovarian Cancer Stages

Ovarian carcinomas are classified by the Féderation Internationale de Gynécologie et d'Obstétrique (FIGO) and the American Joint Committee on Cancer (AJCC)[8]. The FIGO classification system is more often used than the AJCC system[8]. Tumors are classified as stages I through IV[8]. In stage I carcinoma cancer cells or tumor are confined to the ovary, stage II cancer has extended to the pelvic tissues, and stage III involves "histologically confirmed peritoneal implants outside the pelvis, with or without regional lymph node involvement"[8]. Stage IV cancer is characterized by metastasis distant to the pelvis[8].

Tumor types are denoted by their tissue of origin. Four primary cell types give rise to OC: epithelial (the most common), stromal, granulosa, and germ cells[3]. The vast majority (85-95%) of tumors are epithelial derived tumors, with 5 to 8% deriving from stromal cells, 5 to 8% deriving from granulosa cells, and 3-5% from germ cells[3]. Epithelial cell tumors are classified into three subtypes: serous, endometroid, and mucinous[3]. Serous cell layers are comprised of fluid-secreting cells that make up serous membranes[3]. They are the origin of ascites that fills the abdominal cavity that is synonymous with cancer progression. Serous epithelial tumors are the most common, comprising 40% of cases[3]. It is proposed that they originate from the ovarian surface epithelium or cortical inclusion cysts (discussed in the next section)[9]. Endometroid tumors resemble endometrial tissue but form on the ovarian surface epithelium. This classification of tumor makes up 20% of epithelial cancer cases and is divided into two subtypes; tumors with or without endometriosis present[3]. Up to 40% of endometroid

tumors are present bilaterally[3]. The mucinous subtype has an unclear origin, but may occur more often with endometriosis, and is associated with *pseudomyxoma peritonei*, a tumor of the mucous producing cells in the peritoneum[3]. Stromal tumors derive from the granulosa/theca cell layer[10]. Germ cells tumors are normally seen in patients under the age of 18[3].

Tumors are classified based on growth patterns into two types: type I and type II[11]. Type II tumors are classified as "high-grade" while Type I tumors are classified as "low grade"[9]. Type I tumors are distinguished by slow growth, lack of malignancy, and generally found as large masses[12]. Type I growths also harbor specific mutations in *KRAS* (Kirsten rat sarcoma viral oncogene homolog), *BRAF* (a member of the *RAF* kinase family of transcription factors), and *HER2* (human epidermal growth factor receptor 2) genes in approximately two-thirds of ovarian cancers[9]. TP53 gene mutations are less common[9]. Type I carcinomas are typically less lethal due to their inherent lack of malignant transformation and growth pattern[9]. Type II tumors are classified as aggressive, rapidly evolving and genetically distinct from their tissue of origin[12]. They tend to lack the predictable mutations of the type I variety, but instead are genetically unstable and harbor a large number of TP53 gene mutations[9]. Tumors may originate from the ovarian surface epithelium (OSE) or from cortical inclusion cysts (CICs). Cortical inclusion cysts result from epithelial cell implantation into the stigma resulting in inflammation and DNA damage[13]. Damage to the epithelial surface of the ovary following ovulation may give rise to malignant cell types[11]. However, the exact cause of OC is uncertain, and there are several alternative hypotheses in addition to the known sources of ovarian tumors.

Hypothesis of Origin

There are two prevailing hypotheses to explain the origin of human ovarian tumors: the incessant ovulation hypothesis and the extra-ovarian origin hypothesis. The incessant ovulation hypothesis was first proposed by Fathalla in 1971, who postulated that as the number of ovulations during the course of a woman's lifetime increases, so does the risk of OC[14]. At ovulation, minor trauma is introduced to the ovarian surface when it ruptures to release the mature oocyte[15]. As such, the surface epithelium is exposed to inflammatory mediators[16]. It is the resulting damage and repair process that is thought to be the most likely source of carcinogenesis. The ovarian surface is exposed to a high concentration of reactive inflammatory mediators upon rupture of the epithelium[14]. The resulting flood of reactive oxygen species from immune cells reacting to the inflammation damages DNA, which is normally repaired through cellular DNA repair mechanisms, including the action of TP53[14]. In addition, there is damage imparted by ischemia-reperfusion injury that occurs with ovulation, as well as the resulting repair process [17]. Finally, the ovary has the tendency to form an invagination of the epithelial layer, called a cortical inclusion cyst (CIC), after rupturing[18]. Although unclear why, the cysts may continue to be present in the cortex before they regress[18]. It is thought that the presence of these cortical inclusion cysts may contribute to the development of a cancerous phenotype, however the exact mechanism is unknown[18].

The second hypothesis is that ovarian tumors arise from structures outside the ovary including serous fluid-producing epithelial tissue (in serous carcinomas) and the fallopian tubes[19]. It is proposed that ovarian tumors of Müllerian phenotype must first

undergo malignant transformation into a Müllerian-like epithelial tissue[19]. It is noted that this transformation occurs within cortical inclusion cysts of the ovary[19]. This is proposed to occur in part due to exposure of the stigma to estrogen and to other hormones immediately after ovulation, which may impart a metaplastic change in damaged cells[19]. The fact that these cortical inclusion cysts are located deep within the ovarian cortex also lends support to the notion that exposure to ovarian hormones may impart a change in differentiation, as the cortex retains a high concentration of these hormones[19]. Although a transition state from the CIC to a cancerous phenotype has not yet been observed[9], cortical inclusion cysts that closely resemble fallopian tube epithelium are frequently recorded[20].

Human ovarian tumors have been described as originating from the fallopian tube as well[19]. This is supported by observations of the development of ovarian-like tumors in patients years after undergoing salpingo-oophorectomy[19]. Invasive cancer of fallopian tube origin has been documented in women with a family history of OC[9]. Large percentages (~70%) of nonhereditary ovarian tumors are also associated with serous tubal intraepithelial carcinoma (STIC)[9]. STICs are found in the fimbria of the fallopian tube, and it is thought that cancerous cells may migrate to the ovary after detaching from the epithelial layer[9]. STICs from the original tumor have a high rate of TP53 mutation, which is associated with type II OC lesions[9]. They are detected in half of pelvic type II cancers and in approximately 15% of fallopian tubes removed as part of a salpingo-oophorectomy in women with a high risk of OC[20]. The STICs resemble type II ovarian carcinomas morphologically[20].

Therefore, the theory that the multiple subtypes of OC share a common origin is questionable. The more inclusive theory that the differing types of OC have multiple origins has gained support, however publications are increasingly proposing that the reality is a combination of both theories[9]. Indeed, one of the most important challenges in medicine is the development of an early detection method of OC that could account for the number of possible subtypes that exist.

Early Detection of Tumor

Unlike other cancers, a hallmark of OC is the difficulty with which it is detected before metastasis. The ovaries are located deep within the pelvis, making it difficult to detect a tumor upon clinical examination[21]. In addition, OC typically arises later in life, during menopause, when ovarian dysfunction may go unnoticed[21]. Combined with the lack of a sensitive, specific biomarker to use for detection from blood or serum, the result is that most diagnosed cases have progressed past stage II[21]. A biomarker is considered to be useful for diagnostics if it has a minimum positive predictive value (PPV) of 10% and a specificity of 99.6%[21]. The current biomarker used to predict ovarian tumor has a PPV of 69%.[17] This biomarker is CA-125, a glycoprotein that is normally found in tissue derived from coelomic and Müllerian epithelium[21]. CA-125, however, is elevated in numerous other noncancer physiological states, such as pregnancy and menstruation, as well as other cancers, such as breast and colon cancer[4]. CA-125 has also been found in cortical inclusion cysts (CICs), which lends support for the extra-ovarian origin of OC hypothesis[21]. Multi-marker diagnostic methods have been proposed as a way to provide

greater specificity to OC diagnosis[22]. Screening for CA-125 is often combined with transvaginal ultrasound due to its lack of specificity[4].

An investigation to discover new biomarkers by Zhang *et al*.[22] revealed three novel proteins that, when combined with CA-125 analysis, improved the sensitivity and specificity of cancer detection[22]. However, despite this, sensitivity remained at 83% and specificity at 94%, leaving this method still unsuitable for use in screening the general population[22]. A study utilizing age, menopause status, ultrasound, and CA-125 measurement noted an improvement in sensitivity and specificity, however, these levels still remained at 85% and 96%, respectively[21]. A study conducted by Einhorn *et al*.[23] detected OC in six of 175 women with elevated CA-125 concentrations, while 16 tumors of non-ovarian origin were detected in that same group[23]. In addition, three patients were discovered to have ovarian tumors despite exhibiting a normal CA-125 concentration. Therefore, the reliability of the CA-125 biomarker for early diagnosis is questionable.

These results make CA-125 an unsuitable biomarker for OC diagnosis – needless surgeries, expense, and worry on the part of the patient result from a test that is not sensitive or specific enough to detect cancer with certainty. In addition, the prospect of false negatives occurring in the population may leave patients vulnerable to disease.

In an effort to improve screening with the currently available technology, repeated tests have been used to establish a pattern in individual patients, taking into account their age-specific risk of cancer and medical history[21]. Finally, new research is suggesting that proteomic studies may be a method to detect cancer. Surface-enhanced and matrix-associated laser desorption/ionization time-of-flight (SELDI-TOF and MALDI-TOF respectively) analysis have identified 100% of OC cases in preliminary studies[21].

However, this technique is still controversial; the primary criticism is that it detects primarily high-abundance proteins, and that minute changes in the proteome will be unable to be identified [21].

Gallus as a Model of OC

Animal models are extremely important to research in order to understand the biological mechanisms of disease, as well as to invent treatments. Currently, animal models that mimic human OC are difficult to use because there are few that develop OC spontaneously[24]. Animals are, in general, pregnant, lactating, or anovulatory, which are not associated with the development of OC[25]. A limited number of murine models, including Sprague-Dawley rats and some strains of mice, develop ovarian tumors spontaneously[24]. However the rate of incidence is extremely low, making any study with a large number of animals cost-prohibitive[24]. They also display a greater variety of histological subtypes (tubular adenomas, cystadenomas, mesotheliomas) than what is desired for purely OC study; this makes the mouse model even more difficult to use[24]. Using carcinogens or xenografting to induce the formation of a tumor is possible in some instances but can introduce additional variables that make it difficult to determine the origin of a tumor[24]. It also makes it difficult to determine the mechanism of tumor formation. Although primary cell lines taken from tumors or ascites are used in studying OC cell biology, this method does not precisely model what occurs in the human patient.

As mentioned previously, the laying hen (*Gallus gallus*) has begun gaining popularity as a model of ovarian carcinoma[25]. According to the incessant ovulation

hypothesis, there is a positive correlation between the number of ovulations and the development of OC[14]. The laying hen is a regularly ovulating animal that has been shown to develop ovarian malignancies after approximately two years of life at a rate of 25%[25]. The age-related increase in frequency of OC is similar to what has been observed in women. The ovulatory cycle of a hen is similar to that of a human female, and the spread of OC within the body cavity mimics the spread in a human, in both abdominal metastasis and the generation of ascites[25].

Chickens also share similar biomarkers that will cross-react with antibodies made towards human biomarkers, such as epidermal growth factor receptor, cytokeratin, and CA-125[25]. Previous studies have shown that mutations are known to occur in conserved regions of TP53 in laying hens with OC, which is also common to not only OC but many other forms of human cancer as well[26]. These properties make *Gallus* an attractive choice to use for OC study.

Chapter 2

The TP53 Gene

The TP53 gene, located on chromosome 17p13.1 in humans, codes for a 393 (human) or 367 (*Gallus*) amino acid cytosolic phosphoprotein approximately 43kDa in mass[27]. In *Gallus*, the mRNA coding sequence (CDS) is 1,153 bases in length compared to human TP53 at 2,451 bases[27]. Depicted in Figure 2-1, the protein contains an N-terminal transactivation domain and proline-rich region, a central DNA-binding domain, and a C-terminal oligomerization domain[27]. Its primary role is a tumor suppressor, doing so by binding DNA to prevent transcription and allow for repair after damage is incurred, as well as interacting with numerous anti-proliferative pathways involving cell cycle arrest and apoptosis (Figure 2-2)[28]. Mouse model knockouts of TP53 show normal early development, but develop numerous cancers at a rate of 75% by six months[29]. The TP53 gene product is a transcription factor, which modifies the expression of a large number of cellular genes[30]. TP53 responds to a variety of cellular stresses, such as DNA damage from ionizing radiation or reactive oxygen species, hypoxia, oncogenesis, and ER stress (Figure 2-3)[28].

TP53 is chiefly regulated by MDM2 (murine double-minute two), an ubiquitin ligase that binds it at serine residues in the N-terminal transactivation domain to mark it for degradation during periods of non-stress[28]. MDM2 is responsible for keeping concentrations of TP53 nearly undetectable in healthy cells[28]. Tp53 itself is a target of its own transcriptional activation, such that activation of TP53 will negatively feed back to

inhibit itself [28]. The interaction is broken when cellular stresses activate a number of kinases that phosphorylate TP53 to activate its transcriptional activity [28]. TP53 is also negatively regulated to some extent by the ubiquitin ligases P53-Induced Ring H2 (Pirh2) and Alternate Reading Frame Binding Protein I (ARF-BP1), but MDM2 appears to be the primary regulator[31].

TP53 activation classically occurs in three steps: stabilization (removal of inhibition), DNA binding, and activation of transcription[31]. Post-translational modifications are made to TP53 by protein kinases such as Ataxia telangiectasia mutated (ATM), DNA Protein Kinase (DNA-PK), and the Checkpoint Kinases (CHK1/CHK2) in response to various cellular stresses such as damage from UV radiation, DNA double strand breaks, and H_2O_2 (Figure 2-3)[31]. Phosphorylation of serine resides in the N-terminal transactivation domain breaks the association of TP53 with MDM2 and allows it to interact with downstream pathways (Figure 2-2)[31]. TP53 is a functional tetramer that achieves this conformation through its C-terminal oligomerization domains[32]. The TP53 tetramer will stabilize after phosphorylation so it may bind DNA to alter transcription[32]. It is currently not known how TP53 is targeted to stress-specific gene sequences[31]. The N- and C-terminal regions are subject to phosphorylation, but also acetylation, methylation and ubiquitination as a response to different stressors[31]. TP53 interacts with p21, FAS, Bcl-2 Associated X-Protein (BAX), P53-Induced Gene III (PIG3), and P48, among others to carry out its effects of cycle arrest, apoptosis, DNA repair, and inhibition of growth pathways (Figure 2-2)[28].

Mutations in human TP53 are known to occur in roughly 50% of all human cancers[33]. Mutations in the DNA binding domain of TP53 are associated with worse overall survival rate in human breast cancer[34], human colorectal cancer[35], and ovarian carcinoma[36]. In chickens, few studies have been conducted examining the status of TP53 in ovarian carcinoma. A study conducted by Takagi *et al.*[37] detected numerous deletions in the DNA binding domain of *Gallus* mRNA transcript from lymphoblastoid cell lines transformed by Marek's disease virus. A representative deletion is illustrated in Figure 2-4. This demonstrates that viruses such as Marek's disease are capable of introducing mutations that inactivate the TP53 gene[37]. In a separate study, the authors discovered deletions of the DNA binding domain present in chicken cell lines derived from avian sarcoma leukosis virus[38].

Splice site mutations have also been associated with increased cancer formation[39,40]. A study conducted by Surget *et al.*[40] characterized 12 alternative splicing patterns of the TP53 gene (Figure 2-5). While the implications of alternative splicing of TP53 have yet to be fully understood, isoforms missing the domains contained within the N-terminal region (transactivation domain and proline-rich region) are found to be overexpressed in breast tumors and highly angiogenic tumors such as glioblastoma multiforme[41].

Previously discovered deletions of the TP53 mRNA transcript are illustrated in Figure 2-4. In a study comparing two flocks of leghorn hens, Hakim *et al.*[26] discovered numerous mutations in TP53 mRNA transcript of *Gallus domesticus* following ovarian adenocarcinoma that corresponded to the DNA binding domain[26]. The two flocks labeled

A and B exhibited different mutation patterns[26]. Flock A was feed-restricted resulting in cessation of ovulation without starving the animals[26]. Flock B received a normal caloric intake to support daily ovulation[26]. TP53 deletions were found in flock A, but only missense mutations were found in flock B[26]. TP53 mutations were discovered in 48% of *Gallus* ovarian carcinomas from this study, including several deletions in the DNA binding domain[26]. Deletions in this instance occurred in both the DNA binding domain alone (Figure 2-4, line 4) or spanned the DNA binding domain and C-terminal region. Finally, Trtkova *et al*.[38] detected additional deletions in chicken Tp53 in *v-src* transformed cell lines as shown in Figure 2-4, line 5. *V-src* is a cell-transforming virus known to produce sarcoma in chickens[38]. Similar to the effects of Marek's virus, Trtkova *et al*.[38] demonstrated that *v-src* is capable of introducing deletions into the DNA binding domain of the TP53 mRNA transcript early in cell culture. This mechanism of tumor development is supported by the phenomenon of inactivating the remaining full-length TP53 allele after incurring mutations in the other allele[38].

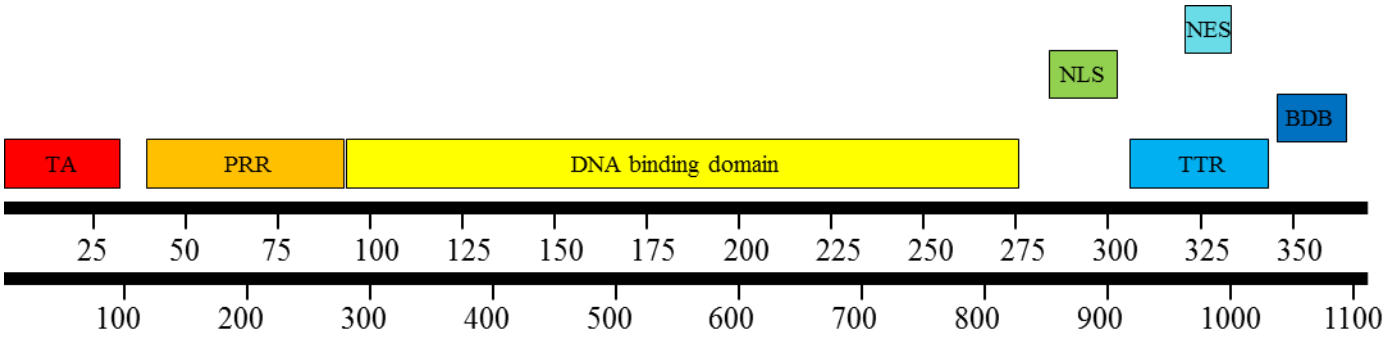

Figure 2-1. Schematic of chicken TP53 Domains. The first numbered line represents amino acid numbers. The second numbered line represents nucleotides in the mRNA transcript. Domain structure was taken from National Center for Biotechnology Information (NCBI). (TA = transactivation domain, PRR = proline-rich region, NLS = nuclear localization signal, NES = nuclear export signal, TTR = tetramerization domain, BDB = basic DNA binding domain). Source: National Center for Biotechnology Information. Cellular tumor antigen p53 (Gallus gallus). 14 May 2014. http://www.ncbi.nlm.nih.gov/protein/46048718?report=graph

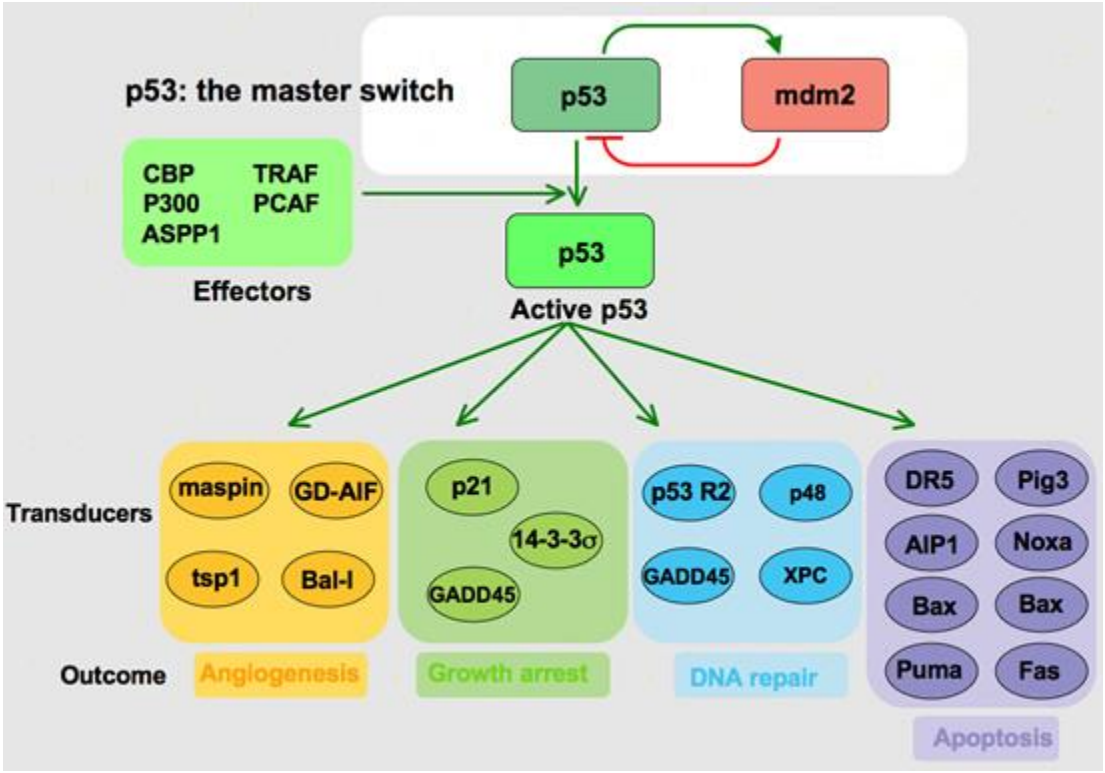

Figure 2-2. Cellular outcomes of TP53 upregulation. While the TP53 protein is normally present at near-undetectable levels in the nucleus and cytosol, cellular stresses result in upregulation of gene expression. "Active" TP53 is the tetrameric protein product and acts as a regulator of angiogenesis, cell cycle arrest, DNA repair, and apoptosis. Source: Soussi, *et al*. 2012. The TP53 Web Site. MASPIN – Mammalian Serine Protease Inhibitor; GADD45 – Growth Arrest and DNA Damage Protein 45; BAX – BCL2 – Associated X-Protein.

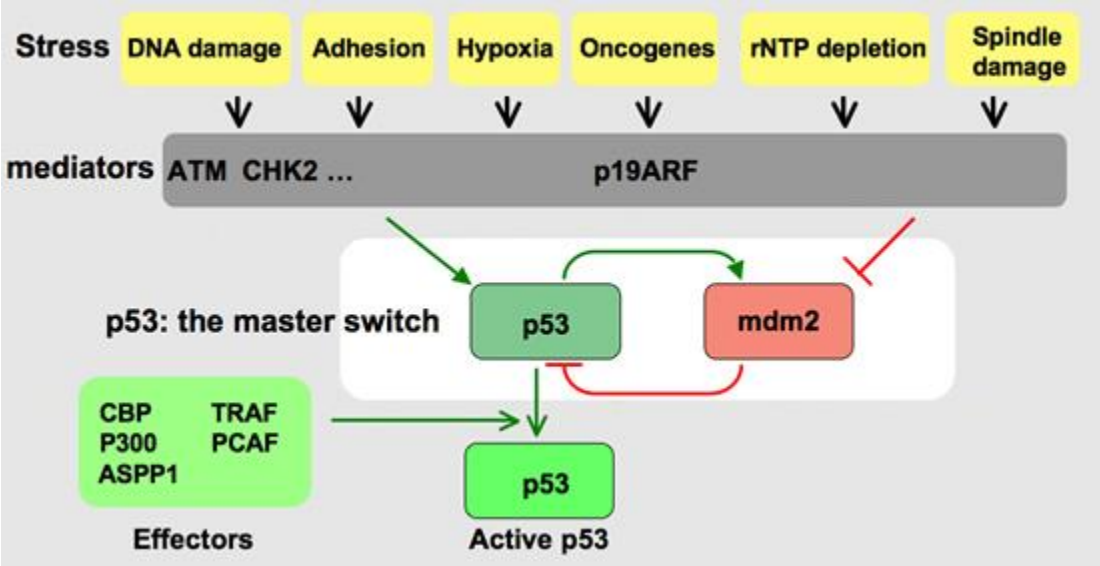

Figure 2-3. TP53 protein expression is upregulated by cellular mediators of stress. DNA damage, cellular adhesion, hypoxia, and others initiate the activation of mediators such as ATM and CHK2, which inhibit the negative regulatory action of MDM2 on TP53, allowing its expression to be upregulated. Source: Soussi, *et al*. 2012. The TP53 Web Site.

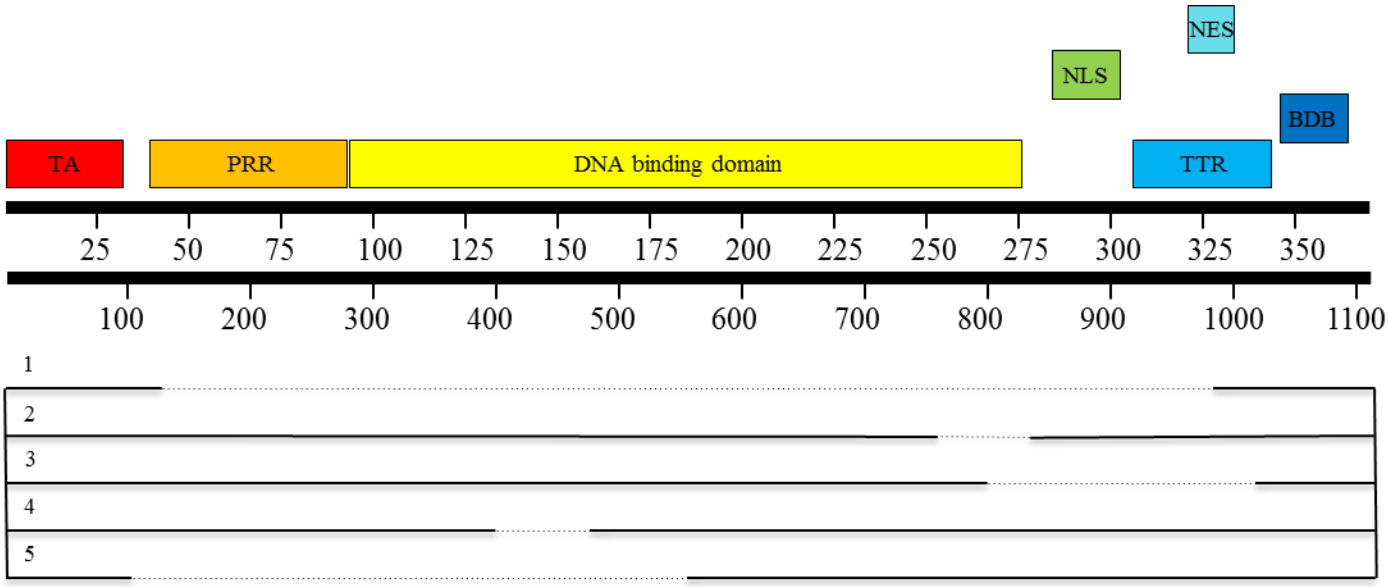

Figure 2-4. Deletions in TP53 mRNA transcript derived from chicken ovarian tumor and virus-infected chicken cell lines. (1) TP53 deletions detected in the presence of Marek's disease virus tumor derived cell lines by Takagi *et al*.[37] (2) 122 BP deletion detected in chicken lymphoblastoid cell lines by Trtkova, *et al*.[38] (3) and (4) Deletions detected in feed-restricted and *ad libitum* fed birds by Hakim *et al*.[26] (5) Deletions detected in *v-src* transformed chick cells by Takagi *et al*.[42] (TA = transactivation domain, PRR = proline-rich region, NLS = nuclear localization signal, NES = nuclear export signal, TTR = tetramerization domain, BDB = basic DNA binding domain).

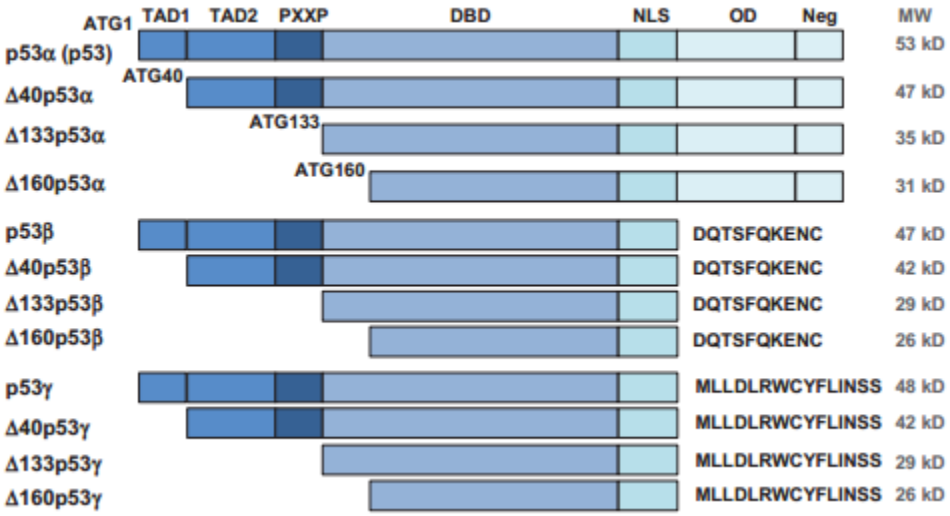

Figure 2-5. Known splice variants found in human TP53 protein. Of the known splice variants that have been detected in human TP53, those of interest to us are the short forms lacking the proline-rich regions (Δ133p53α, β, and γ and Δ160p53α, β, and γ). Previous studies suggest that these forms may create an environment permissible to tumor formation. Source: Surget *et al*.[40] "Uncovering the role of p53 splice variants in human malignancy: a clinical perspective". OncoTargets and Therapy. Dec. 2013.

Objective and Hypothesis

The objective of this study was to determine if the sequence of the TP53 mRNA transcript is different in chickens that have ovarian tumors compared to controls. The hypothesis for this study is that the TP53 mRNA transcript in ovarian tumors and ovarian cancer cell lines will harbor mutations that are not present in healthy controls.

Chapter 3
Methods

White Leghorn hens (W-36 strain, n=24; aged 24-48 months at time of euthanasia) with advanced (stage IV) OC as well as healthy age-matched (n=8) and young (n=5; 5.5 months) control hens were used in this study. Leghorn hens were euthanized by either cervical dislocation or decapitation, according to procedures approved by the Pennsylvania State University Institutional Animal Care and Use Committee. The young Leghorns were included in the study as they had fewer than 20 ovulations and therefore may have less DNA damage in the ovary due to repeated ovulations[15]. Whole ovarian tissue was taken within five minutes of euthanasia, snap-frozen in liquid nitrogen and stored at -80°C. Furthermore, ascites-derived chicken ovarian carcinoma cancer cell lines (COVCAR, n=6, Tiwari et al.[53]), adipose and liver tissue were also utilized for comparison of TP53 mRNA sequences.

Total RNA was extracted and reverse transcribed to cDNA. Ovarian tissue (stroma and ruptured follicle, 0.2 g) was cut with a sterile razor blade and homogenized in 2 mL of Trizol (Ambion, Grand Island, New York) reagent and incubated for five minutes at 23°C (room temperature). Homogenate was transferred to a 50 ml tube and centrifuged at 12,000 x g (Eppendorf, Hauppauge, New York) for five minutes at 4°C. 400 µL of chloroform (Sigma-Aldrich, St. Louis, Missouri) was added and the tube was shaken by hand for 15 seconds. Samples were incubated at room temperature for three minutes and centrifuged at 12,000 x g for 15 minutes at 4°C. The aqueous phase was

transferred to a new 15 ml centrifuge tube, and an equal volume of 70% ethanol (7 ml ethanol**,** Omnipur, 3ml diethylpyrocarbonate (DEPC)-treated water, Invitrogen, Grand Island, New York) was added before transferring to a silica-membrane spin column (Qiagen, Valencia, California), centrifuged for 30 seconds at 10,000 RPM, and transferred to a new tube. DNAse (10 µL; Qiagen) and 70 µL of RDD buffer (Qiagen) were added to each sample. Samples were incubated for 15 minutes at 23°C (room temperature). RW1 (700 µL; Qiagen) was added to each sample and centrifuged as described above. The column was again transferred to a new microcentrifuge tube and 500 µL of RPE (Qiagen) was added and centrifuged for 30 seconds at 12,000 x g. The column was transferred to a new microcentrifuge tube and centrifuged at 16,000 x g for one minute to remove remaining ethanol. RNA was eluted with 30 µL of RNase free water (Qiagen) by spinning for one minute at 12,000 x g. The RNA concentration was determined using a Nanodrop 2000C (Thermo Scientific).

Total RNA was reverse transcribed to cDNA by first adding random primers (Promega, Madison, Wisconsin) and dNTP (Roche, Branchburg, New Jersey) in a microcentrifuge tube. Ultra-pure RNAse-free water (Qiagen) was added to bring the reaction volume to 16 µL. Sample tubes were heated to 95°C for 10 minutes in an MJ Research PTC-200 thermocycler. Sample tubes were removed and immediately placed on ice. RT buffer (10 x; New England Biolabs, Ipswich, Massachusetts) was added at 1X concentration. RNAse out (Invitrogen, Grand Island, New York) and MMLV reverse-transcriptase enzyme were added at 1X concentration (New England Biolabs) to bring the final reaction volume to 20 µL. Samples were incubated in the same thermocycler described earlier under the following conditions: 42°C for 90 minutes, followed by 90°C

for 10 minutes. EDTA (1 mM) (Sigma-Aldrich) and 1 x TE (Omnipur) were added to reaction tubes to dilute cDNA that was subsequently stored at -80°C.

The TP53 transcript was amplified from cDNA using three sets of oligonucleotide primers (PrimerSet1, 2, 3; Table 3-1) that amplified three overlapping regions of the TP53 transcript. A total reaction volume of 20 µL was used. PrimerSet2, PrimerSet3, and dNTPs (Roche) were added at 300 nM concentration. 10 x Advantage PCR buffer (Clontech, Otsu, Shiga, Japan) was added to achieve a 1 x concentration. A 50 x solution of Advantage II mix (Clontech) was added for a final concentration of 1 X. PrimerSet1 was added at 500 nM concentration to increase reaction efficiency. A touch-down PCR was used with the following thermocycling conditions: 94°C for three minutes, 72°C for 15 minutes, 94°C for five seconds, 70°C for three minutes, 94°C for 25 seconds, 68°C for three minutes, 94°C for one minute, 68°C for seven minutes, 35 cycles total. The regions amplified by the primer sets are described in Figure 3-1.

Amplified TP53 DNA transcript was separated via agarose gel electrophoresis. For all samples, a 1% agarose gel was prepared using 1x TAE buffer (Lonza, Walkersville, Maryland) and 50 µL of ethidium bromide. A 6 X DNA loading buffer (New England Biolabs) was added to all samples to a final concentration of 1 X prior to electrophoresis. A 100bp molecular weight ladder (New England Biolabs) was used. Samples were electrophoresed at 80 volts DC for 1.5 hours. Amplified bands were excised via clean scalpel blade and DNA was extracted using a Qiagen DNA cleanup kit (Qiagen). Gel pieces were weighed and a volume of solubilization buffer equal to gel weight in milligrams was added to the microcentrifuge tube. Sample tubes containing gel pieces and DNA solubilization buffer were incubated at 50°C on an Eppendorf

thermomixer for 10 minutes with vigorous mixing every three minutes. A volume of isopropanol (EMD, Temecula, California) equal to the milligram weight of the gel was added to each microcentrifuge tube after incubation and mixed by inverting. The sample volume was added to a silica-membrane column (Qiagen) at room temperature (23°C) and centrifuged at 16,000 x g for one minute. The filtrate was discarded and 500 µL of buffer QG (Qiagen) was added to the column and the column was centrifuged at 16,000 x g for one minute. The filtrate was discarded and 750 µL of buffer PE (Qiagen) was added to the retentate and the column was centrifuged as described above. The filtrate was again discarded and the tube was centrifuged again as described above to remove remaining ethanol from the sample. The column was removed and placed into a clean microcentrifuge tube. DNA was eluted with 30 µL of buffer EB (Qiagen) by pipetting directly onto the center of the membrane, incubating at room temperature for one minute, and centrifuging for one minute as described above. DNA concentration was estimated using a nanodrop spectrophotometer model 1000C.

To verify sequencing data, additional primers were used to amplify the TP53 cDNA. PrimerSet4 amplified a similar region as PrimerSet1 (Figure 3-1). This was used to circumvent the reduction in reaction efficiency encountered when amplifying the GC-rich 5’ region. FwdPrimer5 was used with the reverse primer of PrimerSet2 to produce a large MW cDNA product. Figures 4-1 to 4-7 show the amplification of each primer set. To verify the presence of the spliced transcript, TP53 was amplified from neck adipose tissue and liver. Figure 4-8 and 4-9 show 5’ region amplification of these tissues. For each sample, the visual signal provided by ethidium bromide was faint, but DNA was still recovered at a concentration sufficient to obtain sequencing data. A subset of TP53

partial cDNA was also cloned into PGEM-TEasy plasmid vector (Promega, Madison, Wisconsin) and the resultant clones were sequenced using SP6 and T7 primers.

Amplified TP53 cDNA were sequenced at the Penn State Sequencing Facility using SP6 and T7 primers. Sequences were compared to *Gallus* TP53 (GeneBank, accession #NM_205264) as well as sequences from control animals. Sequence alignment was performed using BLAST program (NCBI).

Table 3.1. Nucleotide sequences of primers used to amplify the TP53 mRNA CDS. Amplified products were taken to be used in qPCR. Annealing temperature remained at 68-72^{0}C to retain stringency. *FwdPrimer5 was used with the reverse primer of PrimerSet2. Agarose gel and PCR data for FwdPrimer5, HCP1 and HCP2 not shown. † Primers Hcp1 and Hcp2 were used by Hakim, et al.[26] that amplified TP53 mRNA in chickens that had ovarian tumor and controls.

Name	Sequence	Range	Expected Product Size	Melting Temperature (^{0}C)
PrimerSet1	Fwd: 5'-TGCACTTACTCCCCGGTGCTGAATAA-3	38 - 444	406	92
	Rev: 5'-TTGCGGAAGTTCTCCTCCTCGATCTT-3'			92
PrimerSet2	Fwd: 5'-GGAACCATTGCTGGAACCCACTGA-3'	350 - 804	454	92
	Rev: 5'-TTCGGCCACGTGCTCTGATTTCTT-3'			91.5
PrimerSet3	Fwd: 5'-CCCATCCTCACCATCCTTACACTGGA-3	731 - 1089	358	91.5
	Rev: 5'-AAAGGCTCGGACTGACCACGCC-3'			92.5
PrimerSet4	Fwd: 5'-TTGCTGGAACCCACTGAGGTCTTCAT-3'	47 - 327	280	91
	Rev: 5'-ACCTTATTCAGCACCGGGGAGTAAGT-3'			88
FwdPrimer5	Fwd: 5'-GGACCTCTGGAGCATGCTCCCCTATA-3	73 - 804*	731	92
Hcp1†	Fwd: 5'-GCGGAGGAGATGGAACCATTG-3'	25 - 317	292	88
	Rev: 5'-GGTCACCTGCACTTACTCCCC-3'			85
Hcp2†	Fwd: 5'-CCCATCCACGGAGGATTATGG-3'	267 - 567	300	87
	Rev: 5'-CGTTACCACGACGACGAGACC-3'			87

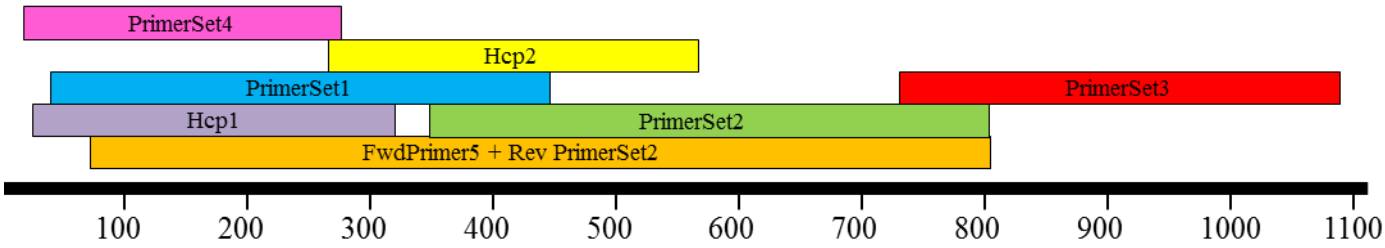

Figure 3-1. Schematic of the TP53 mRNA transcript regions amplified by oligonucleotide primer pairs. Regions are color coded and labeled according to primer set. The position of each amplified region in the cDNA is indicated by the numbered bar. The orange bar used a forward primer designated FwdPrimer5 in combination with the reverse primer of PrimerSet2 to produce a larger PCR product.

Chapter 4

Results

Total RNA from ovarian cancer tissue, COVCAR cell lines, adipose and liver tissue, and healthy age-matched and young chickens was extracted, purified, reverse-transcribed and sequenced. A short form of the TP53 mRNA transcript was detected (Table 4-1). Of the ovarian tissue samples taken from laying hens with advanced OC, all mRNA transcripts sequenced had a 216 base pair deletion spanning nucleotides 115 – 331. The result is a shortened, non-frame-shifted form of the TP53 protein missing 72 amino acids from the TA domain and proline-rich region. The shortened form was present identically in both age-matched and young healthy chickens (Table 4-1). The same deleted form of TP53 mRNA transcript was detected in both liver and adipose tissue taken from hens with OC (adipose data not shown). All COVCAR cell lines tested presented the identical deletion in the TP53 mRNA transcript. The full-length (wild type) form of the TP53 mRNA transcript was not able to be amplified from any tissue or cell culture. A schematic of the deletions is shown in Figure 4-1.

Figure 4-2 is a representative photograph of an agarose gel showing chicken TP53 partial cDNA derived from cancerous ovary. While the bands are of the expected sizes for PrimerSet2 and 3, the PrimerSet1 band is smaller than the expected size of 406 BP due to the truncated TP53 mRNA transcript. Figure 4-3 is a photograph of TP53 partial cDNA derived from COVCAR cell lines. In all cell lines, the bands were visible below the expected 406 BP size. Figure 4-4 shows the result of amplifying PrimerSet2 and 3 using the COVCAR cell lines. The bands appear at the expected sizes. The truncated

TP53 mRNA transcript was present in normal animals as well. Figure 4-5 shows a lower molecular weight product in the normal animals that is identical in molecular weight to the previous tissue samples. TP53 partial cDNA from normal animals using PrimerSet2 and 3 were of the expected size (Figure 4-6). Healthy young birds also exhibited the truncated product of PrimerSet1, shown in Figure 4-7. The products of PrimerSet 2 and 3 from young healthy birds were of the expected size (Figure 4-8). Figure 4-9 shows partial TP53 cDNA taken from liver and adipose tissue of a white leghorn (W-36) with ovarian cancer. Tumor nodules were not detected in either tissue, but the truncated product of PrimerSet1 was still present.

Eight additional PCR methods were used to attempt to amplify the full-length TP53 mRNA transcript and rule out technical errors that could explain the truncated form of TP53. The additional primers (HCP1 and 2) described in Table 3-1 were used. The primer sequences for HCP1 and HCP2 are identical to those used in a study that successfully amplified the full-length TP53 mRNA transcript in 2009[26]. A description of the additional methods used can be found in the appendix and in Table 5-1.

Single nucleotide substitutions were also observed in animals with ovarian cancer (Table 4-1), and were verified through TA cloning of the plasmids. Single nucleotide substitutions did not result in a frame shift in all of the samples. The substitutions did not change the amino acid sequence.

Table 4-1. Mutations characterized according to type, sample, location, frequency, and consequence. The most notable finding is the deleted / spliced portion of the TP53 mRNA transcript. Point mutations were also detected and characterized. The rightmost column indicates the type of sequencing used to confirm the splicing events.

Mutation Type	Sample	Location	Consequence	Sequencing
Deletion	AC5	115 - 331	Deletion of 72 AA from TA / Proline Rich Region	PCR product
Deletion	AC11	115 - 331	Deletion of 72 AA from TA / Proline Rich Region	PCR product
Deletion	AC13	115 - 331	Deletion of 72 AA from TA / Proline Rich Region	PCR product
Deletion	AC16	115 - 331	Deletion of 72 AA from TA / Proline Rich Region	PCR product
Deletion	AC19	115 - 331	Deletion of 72 AA from TA / Proline Rich Region	PCR product
Deletion	AC6	115 - 331	Deletion of 72 AA from TA / Proline Rich Region	PCR product
Deletion	C5	115 - 331	Deletion of 72 AA from TA / Proline Rich Region	TA Clone + PCR
Deletion	C6	115 - 331	Deletion of 72 AA from TA / Proline Rich Region	TA Clone + PCR
Deletion	C7	115 - 331	Deletion of 72 AA from TA / Proline Rich Region	TA Clone + PCR
Deletion	C9	115 - 331	Deletion of 72 AA from TA / Proline Rich Region	TA Clone + PCR
Deletion	C10	115 - 331	Deletion of 72 AA from TA / Proline Rich Region	TA Clone + PCR
Deletion	C11	115 - 331	Deletion of 72 AA from TA / Proline Rich Region	TA Clone + PCR
Deletion	C12	115 - 331	Deletion of 72 AA from TA / Proline Rich Region	PCR product
Deletion	C14	115 - 331	Deletion of 72 AA from TA / Proline Rich Region	PCR product
Deletion	C15	115 - 331	Deletion of 72 AA from TA / Proline Rich Region	PCR product
Deletion	C16	115 - 331	Deletion of 72 AA from TA / Proline Rich Region	PCR product
Deletion	C17	115 - 331	Deletion of 72 AA from TA / Proline Rich Region	TA Clone + PCR
Deletion	C18	115 - 331	Deletion of 72 AA from TA / Proline Rich Region	PCR product
Deletion	C20	115 - 331	Deletion of 72 AA from TA / Proline Rich Region	PCR product
Deletion	C21	115 - 331	Deletion of 72 AA from TA / Proline Rich Region	PCR product
Substitution	AC6	375	Silent G>A	TA Clone + PCR
Substitution	AC6	402	Silent G>C	TA Clone + PCR
Substitution	AC11	786	Silent A>C	TA Clone + PCR
Substitution	AC13	402	Silent G>C	TA Clone + PCR
Substitution	AC15	402	Silent G>C	TA Clone + PCR
Substitution	C7	786	Silent A>C	TA Clone + PCR
Substitution	C7	828	Silent C>G	TA Clone + PCR
Substitution	C7	864	Silent C>A	TA Clone + PCR
Substitution	C8	402	Silent G>C	TA Clone + PCR
Substitution	C13	402	Silent G>C	TA Clone + PCR
Substitution	C17	402	Silent G>C	TA Clone + PCR
Deletion	N1	115 - 331	Deletion of 72 AA from TA / Proline Rich Region	TA Clone + PCR
Deletion	N2	115 - 331	Deletion of 72 AA from TA / Proline Rich Region	PCR product
Deletion	N3	115 - 331	Deletion of 72 AA from TA / Proline Rich Region	PCR product
Deletion	N4	115 - 331	Deletion of 72 AA from TA / Proline Rich Region	PCR product
Deletion	N5	115 - 331	Deletion of 72 AA from TA / Proline Rich Region	PCR product
Deletion	N6	115 - 331	Deletion of 72 AA from TA / Proline Rich Region	PCR product
Deletion	N7	115 - 331	Deletion of 72 AA from TA / Proline Rich Region	PCR product
Deletion	N8	115 - 331	Deletion of 72 AA from TA / Proline Rich Region	PCR product
Deletion	NY1	115 - 331	Deletion of 72 AA from TA / Proline Rich Region	PCR product
Deletion	NY2	115 - 331	Deletion of 72 AA from TA / Proline Rich Region	PCR product
Deletion	NY3	115 - 331	Deletion of 72 AA from TA / Proline Rich Region	PCR product
Deletion	NY4	115 - 331	Deletion of 72 AA from TA / Proline Rich Region	PCR product
Deletion	NY5	115 - 331	Deletion of 72 AA from TA / Proline Rich Region	PCR product
Deletion	Adipose	115 - 331	Deletion of 72 AA from TA / Proline Rich Region	TA Clone + PCR
Deletion	Liver	115 - 331	Deletion of 72 AA from TA / Proline Rich Region	TA Clone + PCR

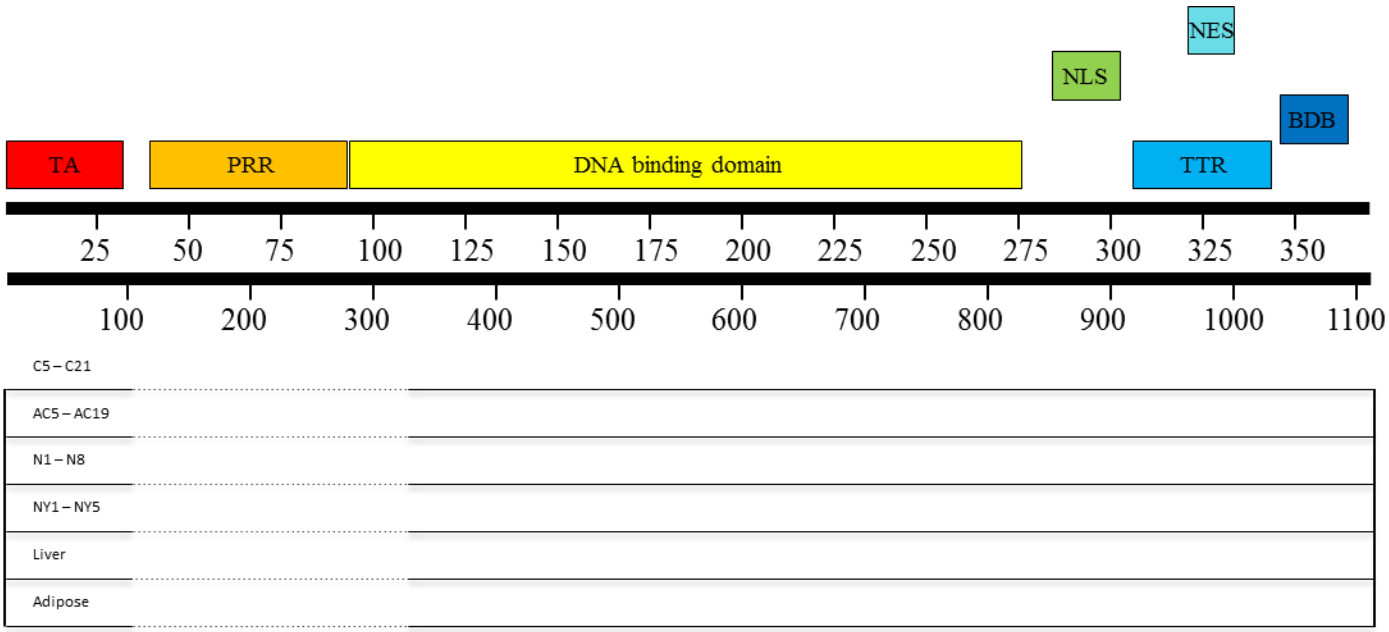

Figure 4-1. Schematic of deletions in chicken TP53 mRNA transcript relative to the TP53 domains. Splicing events present in the mRNA transcript were found to span the 5' end containing the TA domain (shown in red) and the proline-rich region (shown in orange). The 3' end contains the NLS, TTR, NES, and BDB. The first line below domain designations is the numbered amino acid sequence. The second line is the numbered nucleotide sequence of the mRNA. The spliced sequences were confirmed with sequencing data from both PCR and TA cloned samples. C5 – C21 represent ovarian tumor, AC5 – AC19 represent COVCAR cell lines, N1 – N8 represent age-matched healthy controls, NY1 – NY5 represent young healthy controls. (TA = transactivation domain, PRR = proline-rich region, NLS = nuclear localization signal, NES = nuclear export signal, TTR = tetramerization domain, BDB = basic DNA binding domain).

.

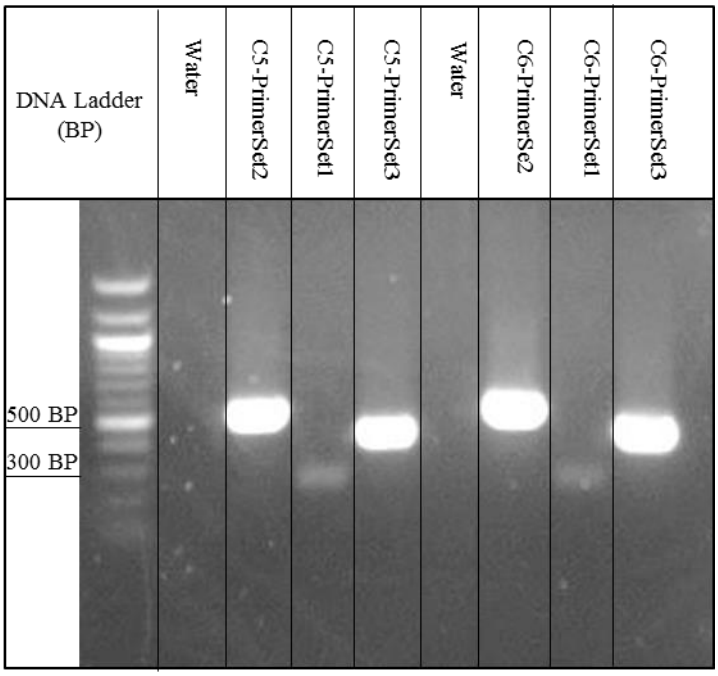

Figure 4-2. Representative photograph of agarose gel showing chicken TP53 partial cDNA. RNA was extracted from cancerous ovary from two animals (C5, C6) and reverse transcribed to cDNA. The partial TP53 transcript was amplified with the three primer sets as shown in the figure. The expected product size of PrimerSet1 is 406 base pair (BP) but only a 288BP shorter form was observed. The expected sizes of PrimerSet2 and PrimerSet3 are 454BP and 358BP, respectively. PrimerSet1 amplifies the 5' TA domain and proline-rich region (nucleotides 38 – 444), PrimerSet2 amplifies the DNA binding domain (nucleotides 350 - 804) and PrimerSet3 amplifies the 3' domains (nucleotides 731 - 1153). Water was used in place of cDNA as a negative control.

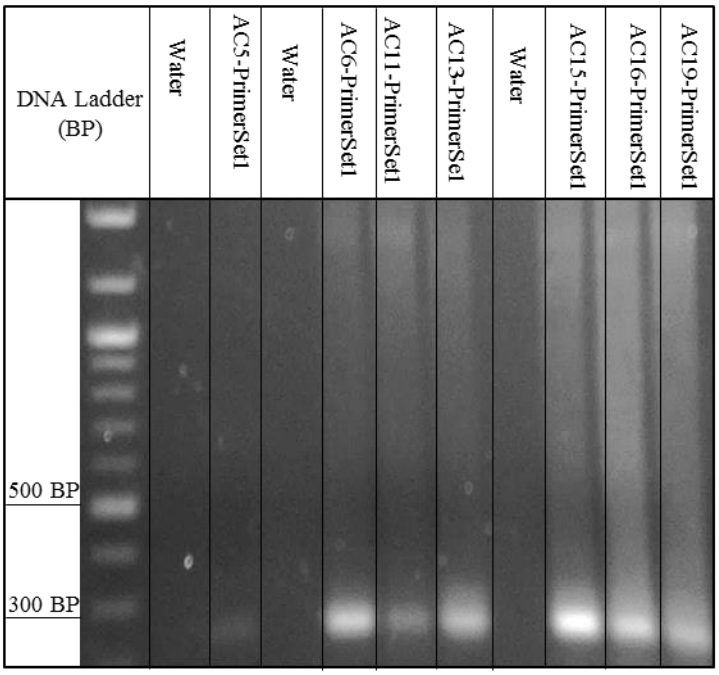

Figure 4-3. Representative photograph of agarose gel showing TP53 partial cDNA expressed in ascites-derived chicken ovarian cancer (COVCAR) cell lines. RNA was extracted from seven COVCAR cell lines (AC5,-6,-11,-13,-15,-16,-19) and reverse transcribed to cDNA. The partial TP53 transcript was amplified with the primer set as shown in the figure. The expected product size of PrimerSet1 is 406 base pair (BP) but only a 288BP shorter form was observed. PrimerSet1 amplifies the 5' TA domain and proline-rich region (nucleotides 38 – 444). Water was used in place of cDNA as a negative control.

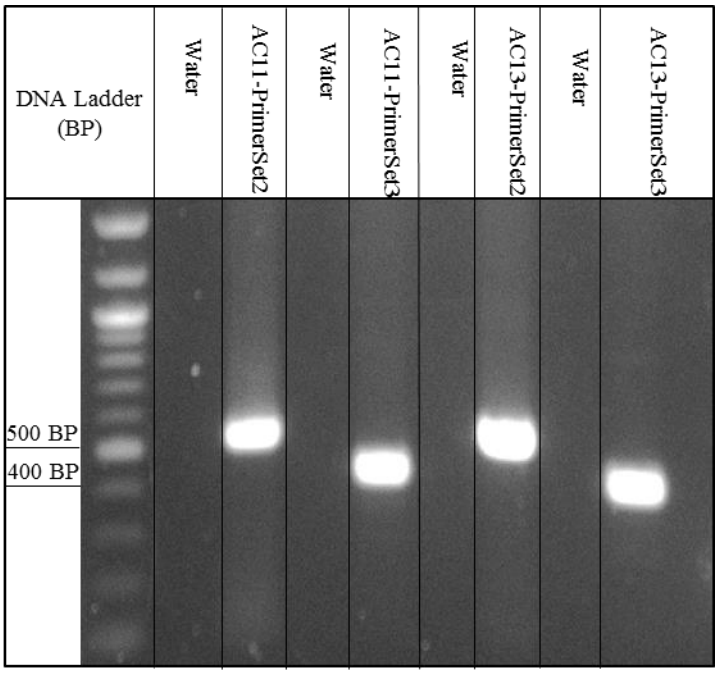

Figure 4-4. Representative photograph of agarose gel showing TP53 partial cDNA expressed in ascites-derived chicken ovarian cancer (COVCAR) cell lines. RNA was extracted from two COVCAR cell lines (AC11, AC13) and reverse transcribed to cDNA. The partial TP53 transcript was amplified with the two primer sets as shown in the figure. The expected sizes of PrimerSet2 and PrimerSet3 are 454BP and 358BP, respectively. PrimerSet2 amplifies the DNA binding domain (nucleotides 350 - 804) and PrimerSet3 amplifies the 3' domains (nucleotides 731 - 1153). Water was used in place of cDNA as a negative control.

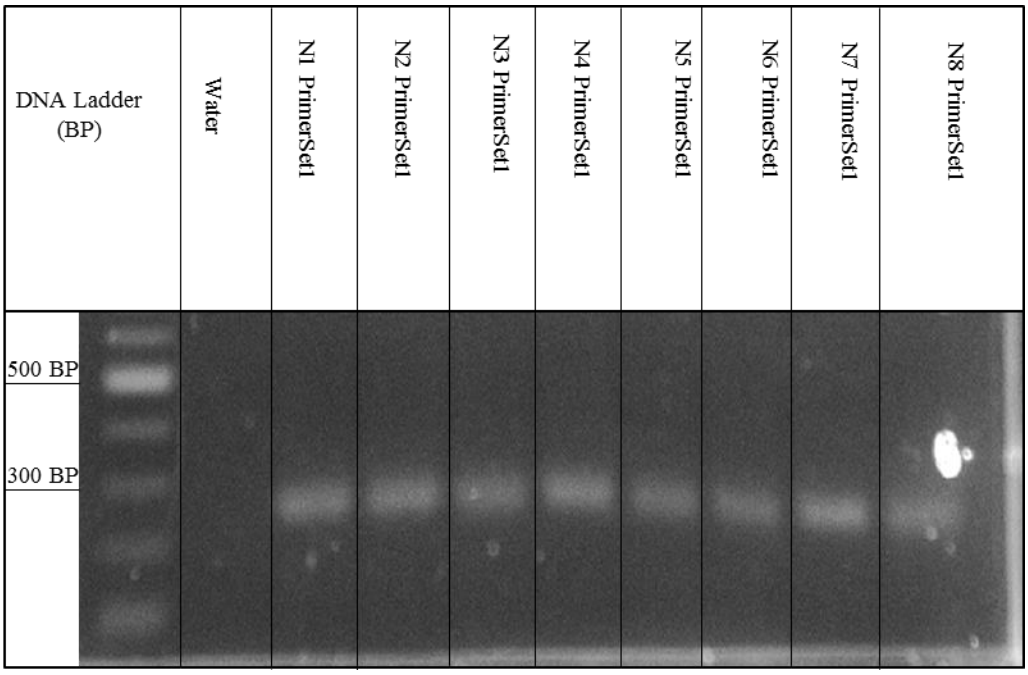

Figure 4-5. Representative photograph of agarose gel showing chicken TP53 partial cDNA. RNA was extracted from age-matched, healthy ovary from eight animals (N1 – N8) and reverse transcribed to cDNA. The partial TP53 transcript was amplified with the primer set as shown in the figure. The expected product size of PrimerSet1 is 406 base pair (BP) but only a 288BP shorter form was observed. PrimerSet1 amplifies the 5' TA domain and proline-rich region (nucleotides 38 – 444). Water was used in place of cDNA as a negative control.

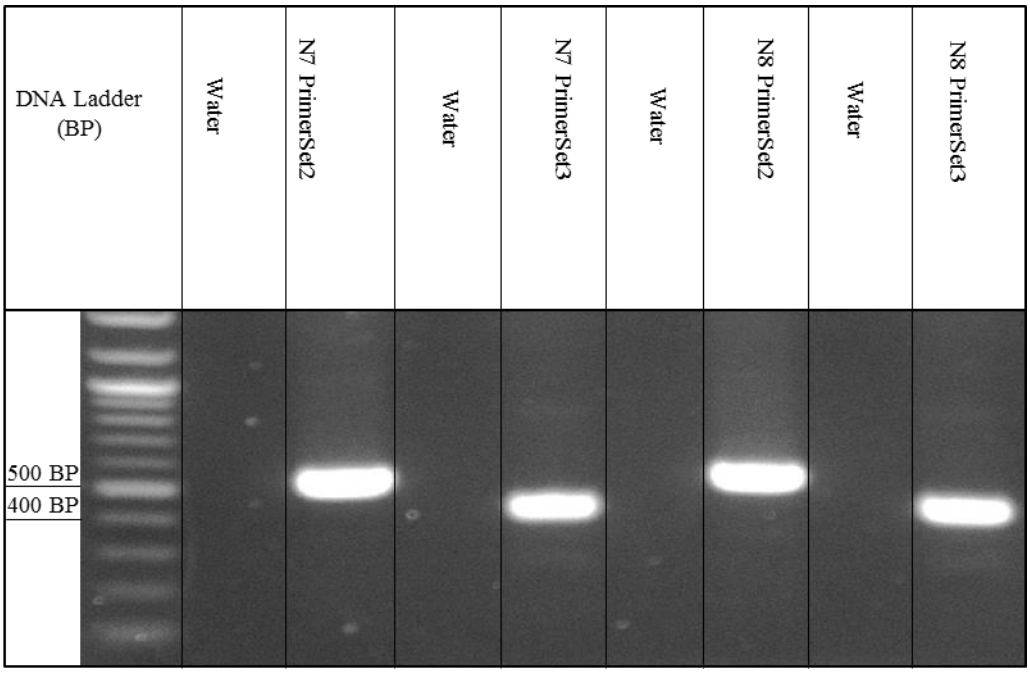

Figure 4-6. Representative photograph of agarose gel showing chicken TP53 partial cDNA. RNA was extracted from age-matched, healthy ovaries from two animals (N7, N8) and reverse transcribed to cDNA. The partial TP53 transcript was amplified with the two primer sets as shown in the figure. The expected sizes of PrimerSet2 and PrimerSet3 are 454BP and 358BP, respectively. PrimerSet2 amplifies the DNA binding domain (nucleotides 350 - 804) and PrimerSet3 amplifies the 3' domain (nucleotides 731 - 1153). Water was used in place of cDNA as a negative control.

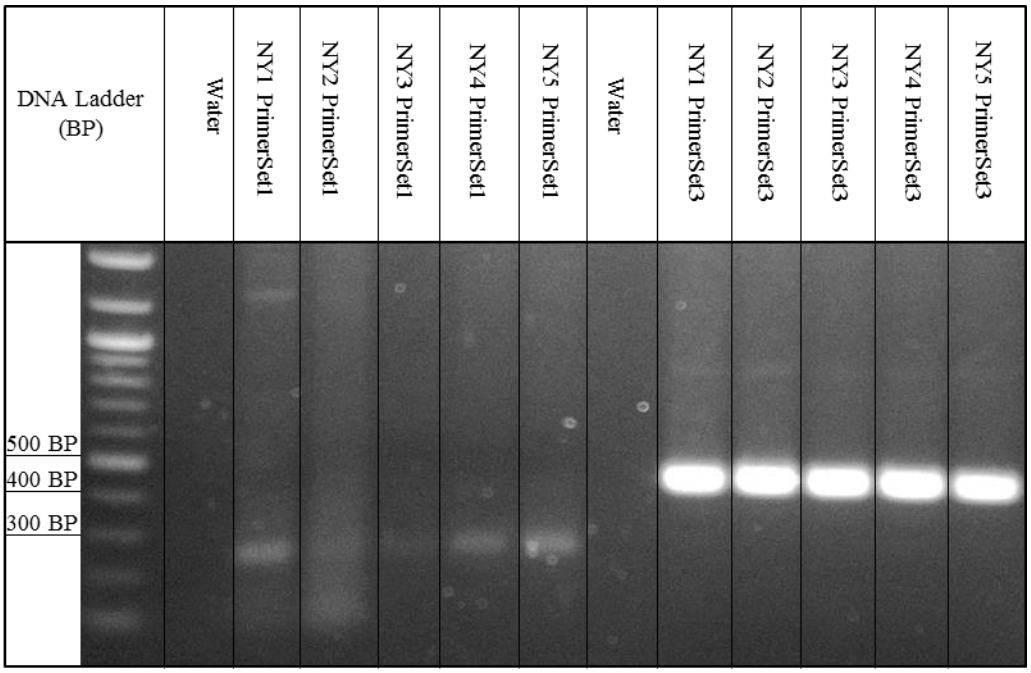

Figure 4-7. Representative photograph of agarose gel showing chicken TP53 partial cDNA. RNA was extracted from young healthy ovaries from five animals (NY1 – NY5) and reverse transcribed to cDNA. The partial TP53 transcript was amplified with the two primer sets as shown in the figure. The expected sizes of PrimerSet1 and PrimerSet3 are 406BP and 358BP, respectively. PrimerSet1 amplifies the 5' TA domain and proline-rich region (nucleotides 38 – 444) and PrimerSet3 amplifies the 3' domains (nucleotides 731 - 1153). The expected product size of PrimerSet1 is 406 base pair (BP) but only a 288BP shorter form was observed. Water was used in place of cDNA as a negative control.

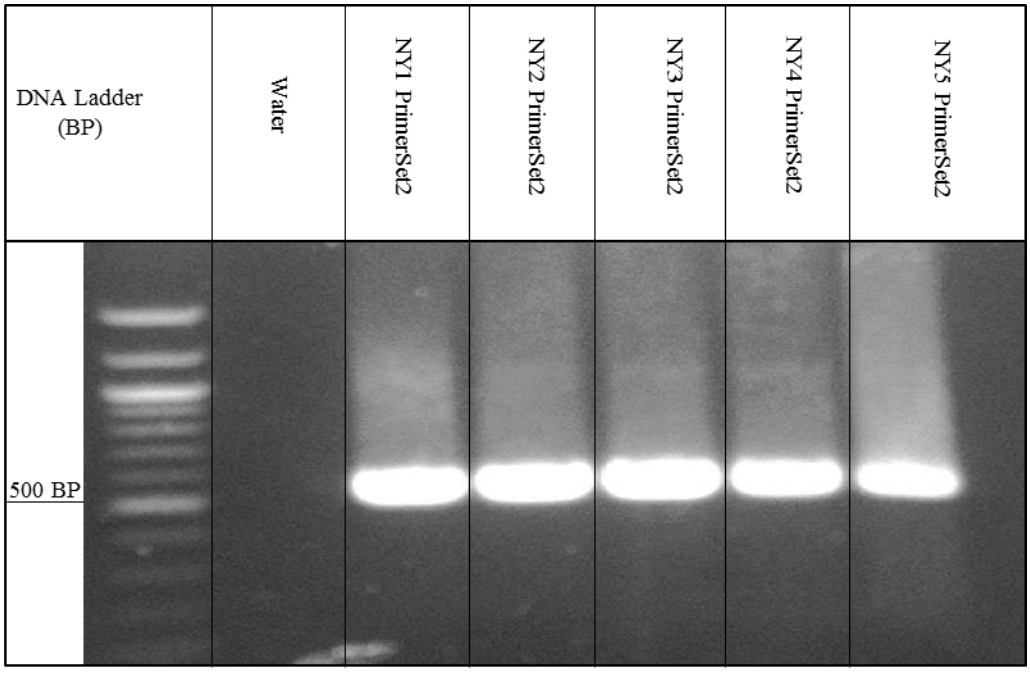

Figure 4-8. Representative photograph of agarose gel showing chicken TP53 partial cDNA. RNA was extracted from young healthy ovaries from five animals (NY1 – NY5) and reverse transcribed to cDNA. The partial TP53 transcript was amplified with the primer set as shown in the figure. The expected size of PrimerSet2 is 454BP. PrimerSet2 amplifies the DNA binding domain (nucleotides 350 - 804). Water was used in place of cDNA as a negative control.

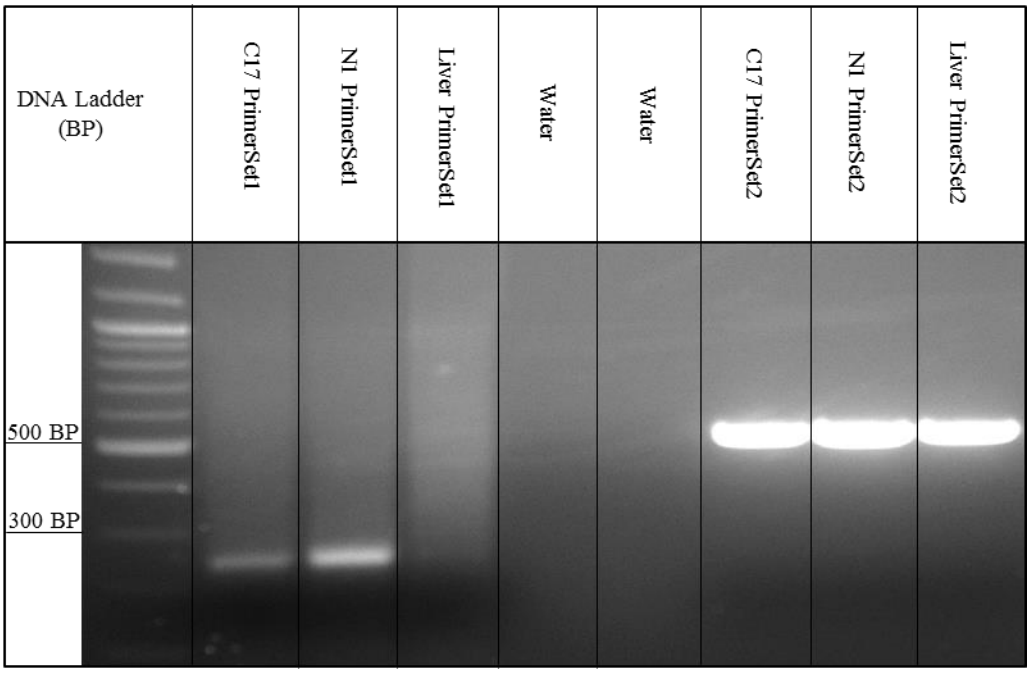

Figure 4-9. Representative photograph of agarose gel showing chicken TP53 partial cDNA. RNA was extracted from cancerous ovary from one animal (C17), age-matched healthy ovary from one animal (N1), and healthy liver from one animal with ovarian cancer (liver) and reverse transcribed to cDNA. The partial TP53 transcript was amplified with the two primer sets as shown in the figure. The expected product size of PrimerSet1 is 406 base pair (BP) but only a 288BP shorter form was observed. The expected size of PrimerSet2 is 454BP. PrimerSet1 amplifies the 5' TA domain and proline-rich region (nucleotides 38 – 444); PrimerSet2 amplifies the DNA binding domain (nucleotides 350 - 804). Water was used in place of cDNA as a negative control.

Chapter 5

Discussion

A truncated form of TP53 mRNA was detected in this study. This mRNA was missing nucleotides 115 – 331 in White Leghorn hens resulting in a shorter TP53 protein. This shortened form of TP53 was detected in all White Leghorn ovarian tumor, liver, adipose tissue, COVCAR cell lines, and interestingly healthy age-matched and young hens. Deletion of nucleotides 115-331 did not result in a frame shift but lead to a shorter form of TP53 protein that lacks part of the TA domain and the entire proline-rich region. Single nucleotide mutations were also detected in ovarian tumor samples; these mutations were silent and did not result in a change in the amino acid sequence. To our knowledge, this is the first time that deletions of the transactivation and proline-rich region have been detected in the chicken model of OC. The normal form of TP53 mRNA as reported in the NCBI GeneBank database (accession #NM_205264) could not be amplified in the present study. A discussion of this is presented at the end of this chapter.

The TP53 tumor suppressing protein is commonly mutated in many forms of cancer. Previous studies have detected mutations primarily in the DNA binding domain of the *Gallus* TP53 mRNA transcript[42]. The most commonly encountered mutations in *Gallus* are single nucleotide substitutions and deletions of the DNA binding domain or 3'- end[26,38,42]. While previous literature describes many kinds of TP53 mutations in ovarian tumors, as well as single nucleotide substitutions in the *Gallus* CDS, there has been only one example of deletions occurring in the transactivation and proline-rich regions. These occurred in cell lines derived from Marek's disease induced tumors[37].

Deletions of the DNA binding domain have also been detected in v-src-transformed chicken embryo fibroblasts[38]. In a mouse tumor xenograft of human glioblastoma, the proline-rich region was found to be required for suppression of angiogenesis[41]. Deletions discovered directly from cancerous ovarian tissue in White Leghorns has not been documented previously. Interestingly, there are several isoforms of the TP53 protein documented in humans that are differentially expressed in normal tissues and tumors (Figure 2-5). The isoforms are splice variants of the full-length TP53 protein and are hypothesized to carry out similar functions to the wild-type TP53.

We have detected a form of TP53 mRNA missing part of the TA domain and proline-rich region. This does not match known isoforms of TP53[40]. The form here is similar to a known isoform of human TP53 missing the transactivation and proline-rich region described previously[43]. Overexpression of this isoform is known to be defective in inducing apoptosis compared to wild type TP53[43]. The study in which deletions in the TP53 mRNA transcript specific to Marek's tumor derived cell lines concluded that the alterations were a result of complex alternative splicing and that no deletions could be detected in the gene itself as revealed by the Southern blot method[37]. Similarly, we believe that what appears as a deletion in this study may be the result of alternative splicing. The truncated sequence of the TP53 mRNA transcript was detected in ovary tissue taken from normal and cancerous White Leghorns as well as adipose and liver tissue of the same animals. It is known that Marek's disease virus produces such changes, but to date no transcripts identical to ours have been recorded. As this virus is capable of creating truncated TP53 transcripts it is possible that a similar event may have produced a spliced transcript in the White Leghorns used for this study.

Genomic Data and the TP53 mRNA Transcript

We believe that the evidence shown here supports our hypothesis that deletions in the TP53 mRNA transcript were caused by one or many splice site mutations. The presence of the shortened form of TP53 in tissues taken from young, healthy birds in addition to ovarian tumors indicates that a splice site mutation may be the cause. Additionally, identical shortened TP53 mRNA transcripts taken from adipose and liver tissue unaffected by tumor suggests that the mechanism may be caused by a virus such as Marek's disease. Our ability to investigate this is hampered by the lack of *Gallus gallus* TP53 genome data. The latest assembly of the chicken genome (galgal4, Feb. 2014) does not contain the TP53 sequence. Furthermore, information concerning *Gallus* TP53 mRNA is also limited. The TP53 mRNA sequence available in the NCBI GeneBank (accession #NM_205264) is derived from specific pathogen free (Spafa) chicken spleen[44]. While this may reflect a wild-type form of the TP53 mRNA transcript, commercial chicken strains are not raised in the same conditions. Germline mutations passed from generation to generation may result in alternative splicing brought on by various viral pathogens, and the TP53 mRNA present in commercial strains of *Gallus* may differ from that of Spafa chicken. Only the White Leghorn strain (W-36) was used in this study. While the mechanism of the deletions has not yet been fully explained[37], we believe that the established cause is a splice site mutation which is supported by its presence in tissue unrelated to the ovary.

Alternative Splicing of the TP53 mRNA Transcript

Alternative splicing of the TP53 DNA binding domain in the context of cancer has been described previously[39]. We cannot determine if the deletions discovered here are genomic in origin. In light of this, we analyzed mRNA from alternative tissues unrelated to the ovary that did not exhibit tumor formation. The shortened form of TP53 mRNA transcript was detected in both liver and adipose tissue of hens exhibiting advanced OC. Splicing mutations of TP53 have been previously described in *Gallus* in several studies[37,38]. The Marek's disease virus belongs to the herpes virus family of viral pathogens and is known to cause malignant lymphomas in *Gallus*[45]. Hens infected with Marek's disease virus exhibit TP53 mRNA transcript that harbors deletions in the DNA binding domain[37]. Several cell lines from tumors caused by Marek's disease were found to harbor large deletions in the DNA binding domains of the TP53 mRNA transcript[37]. Deletions in chicken TP53 are not limited to Marek's derived cancers. A previous study detected deletions in the early passages of immortal *v-src* derived tumor cell lines[38]. *V-src* is known to initiate immortal transformation of chicken cell lines concordant with TP53 inactivation[38]. Deletions spanning several hundred base pairs in the DNA binding domain of TP53 mRNA transcript were detected in chicken sarcoma-derived cell lines[38]. The mutations detected exhibited a high variance that was observed in the earliest passages of the cell lines[38].

TP53 mutations have been detected in tissues taken directly from hens with cancer in addition to immortal cell lines. A study conducted using laying hens harboring ovarian adenocarcinomas discovered numerous deletions in the TP53 mRNA transcript[26].

The deletions were detected within the DNA binding domain in addition to missense mutations discovered in the proline-rich region[26].

The truncated form was the only TP53 form detected in any sample in our study. This does not rule out the full-length TP53 mRNA being present in the ovary or other tissues, though it was undetectable in this study. Numerous alternative splicing variants of TP53 are also described a variety of normal human tissues[43]. To date, 12 different TP53 isoforms have been recorded[40]. Thus, there is a strong possibility that splice site alterations could exist in a chicken model. In general, the short arm of chromosome 17 where TP53 is located is deleted in a majority of human cancers[46]. Mutations on the remaining allele of TP53 are often found[47]. In a study of P53 mutations in patients with advanced colorectal cancer, sarcoma, ovarian cancer, and melanoma, over 80% of deletions of TP53 were located in the DNA binding domain or 3' end[33]. Human osteosarcoma and non-small-cell lung carcinoma cell lines have been demonstrated to lose their ability to undergo programmed cell death upon deletion of the proline-rich region. In breast tissue, two isoforms of TP53 lacking the TA domain and proline-rich regions are overexpressed in 40% of cases[40]. Renal cancers overexpress these isoforms compared to healthy tissues[40]. This indicates that deletions found in TP53 are likely contributing to tumor development. While these isoforms have yet to be fully explored in the *Gallus* model, it lends support to our hypothesis.

Consequence of Truncated TP53 mRNA Transcript

As shown in Table (4-1), the deletions discovered in the present study are located in the transactivation and proline-rich domains. The transactivation domain carries out its function using serine residues that interact with downstream signaling proteins[48]. The deletion described here did not affect any serine residues in the transactivation domain, which abuts the proline-rich region. The proline-rich region is defined by the repeat of the PXXP motif; two proline residues flanking any two amino acids[49]. This region is a domain necessary to TP53 function that transduces signals by interacting with SH3 binding domains in downstream proteins[49]. It has been shown to be dispensable for cell cycle arrest inhibition[49]. The loss of this region (specifically the five PXXP motifs) has been demonstrated to reduce apoptotic activity[49,50]. While the mechanism for cell cycle arrest is well known as being mediated through transcriptional activation of the p21 gene, which prevents the formation of G1 cyclin/CDK complexes, the mechanism of the apoptotic response has not been fully described[51]. Additionally, cell type or environment may play a role in whether or not transcriptional activation is required for apoptosis[51]. It is thought that the loss of this domain prevents reactive oxygen species production required for apoptosis, as demonstrated in both human non-small cell lung cancer (H1299) cell lines[49]. However, the proline-rich domain is not essential for G1 growth arrest[49], and is distinct from the C-terminal domain's role in transcriptional activation[51]. As DNA damage will induce TP53 expression, this may still lead to cell cycle arrest or apoptosis through signaling using the proline-rich region. The proline-rich region

interacts with several proteins such as BAX that signal for apoptosis; dampening this response may allow the cell to bypass apoptosis and continue to grow.

The tissues and cell lines described in this study had a TP53 mRNA transcript lacking the proline-rich region. This may have contributed to the development of ovarian cancer in our White Leghorn hens. Over time the truncated form that we detected in healthy young White Leghorns may not be able to compensate for accumulated DNA damage incurred by repeated ovulation. A previous study, using chemotherapeutic agents to induce TP53-mediated apoptosis, reported that mutant cells lacking a TP53 proline-rich region were completely incompetent at undergoing apoptosis in response to DNA damage caused by chemotherapeutic agents[51]. The existence of the truncated form in both COVCAR cell lines and ovary tissue samples supports the proline-rich region mechanism of uncontrolled growth. However, the response that induces apoptosis remains complex and is likely not able to be attributed to one type of mutation. Phosphorylation of Ser46 is associated with a factor AIP1 that induces mitochondrial apoptosis[51]. Serine residues in the proximal transactivation domain of the mutated genes in our study were not affected. It is possible, therefore, that both of these residues in the transactivation domain and the proline-rich region are responsible for cooperatively inducing apoptosis. In addition, deletion of the proline-rich region has been demonstrated to have an effect on some, but not all apoptotic genes[52].

Several of these apoptotic factors involved in programmed cell death including BAX and PIG3 have been shown to remain functional despite a proline-rich region deletion[52]. In a mouse model of deletion, removal of residues 75-91 resulted in apoptosis occurring only at high levels of DNA damage, while deletion of residues 58-88 caused

complete inability to become apoptotic[53]. In the same study, TP53 response occurred with some stressors (oxidative damage), but not all (ionizing radiation)[53]. Due to the proline-rich region's interactions with the binding sites of downstream molecules such as ATM, the deletion may prevent these sites from being activated[53]. As TP53 can be regulated in a variety of ways, the loss of the proline-rich region may not directly be causing tumorigenesis, therefore other cancer triggers may need to be present.

Two primary downstream signaling molecules involved in the apoptotic pathway, BAX (Bcl2-associated x-protein) and PIG3 (P53-inducible gene), interact directly with the proline-rich region[30]. Our evidence suggests that a loss of these interactions may prevent the TP53 pathway from shifting towards apoptosis after DNA damage. Other post-translational modifications and interactions with apoptotic and inflammatory transcriptional activators may reduce the ability of TP53 to engage downstream pathways for DNA repair or apoptosis, as these pathways are understood to interact with TP53 within the region of deleted residues found in our samples[48]. The negative regulation of TP53 may be affected as well. Janus Kinase, or JNK, acts as an MDM2-independent regulator of TP53. Its function does not have any known interactions with the MDM2 regulation feedback loop of TP53. The loss of the JNK phosphorylation site may reduce the cells' ability to upregulate TP53 in response to cellular stresses[48]. Therefore, mediators of apoptosis and their response to increasing cellular levels of mutated TP53 may be dampened.

In light of the varying responses that TP53 DNA repair can take depending on the specific mutation, it is reasonable to suggest that the truncated form of TP53 may not cause tumorigenesis directly. As suggested by the incessant ovulation hypothesis, the

DNA repair mechanism may not be able to cope with high levels of damage accumulated over time. This is reflected in our detection of the truncated form of TP53 in both age-matched and young normal hens; neither of which exhibited clinical signs of OC. Rather; the truncated form may be a result of alternative splicing incurred by genetic mutations as a result of Marek's disease or related virus.

TP53 mRNA Secondary Structure and its Implications

We believe that the deletion described in this study is the result of alternative splicing events. However, the structure of the TP53 mRNA transcript gives rise to the possibility of PCR artifacts. The *Gallus* TP53 mRNA transcript is composed of guanine and cytosine residues to the extent of 69%. This results in extensive pairing between the mRNA nucleotides. Numerous hairpin loops are formed in GC rich areas where the deletion has occurred between nucleotides 115 – 331. The secondary structure of the 5'-end mRNA is shown in Figure 5-1. Oligonucleotide primers used in these areas may have skipped portions of nucleotides that have formed hairpin loops leaving gaps in the sequence that appear to be deletions (Figure 5-2). We do not believe this to be the case because we have encountered identical sequences across all samples and confirmed this with TA cloning and sequencing of plasmids containing TP53 cDNAs. Additionally, our PCR reaction conditions (described previously) were designed to eliminate hairpin loops.

Conclusion

Ovarian cancer is the most deadly of the gynecological cancers. There is no reliable method of prediction or viable animal model. The *Gallus* model of OC is promising as laying hens develop ovarian cancer at a rate of 25% after two years, and the spread of OC in chickens mimics that of humans. In addition, it shares 72% identity with the human TP53 CDS, a tumor suppressing gene commonly mutated in human cancers.

A transcription factor that is expressed during cellular stress, the TP53 gene is commonly referred to as the "guardian of the genome" [31]. It functions in multiple roles such as cell cycle arrest, apoptosis, DNA repair, metabolism, and senescence[31]. Mutations in the TP53 DNA binding domain are commonly found in human cancers, including ovarian, breast, and colorectal cancer.

In this study, we sequenced TP53 cDNA derived from healthy age-matched and young chicken ovary, ovarian tumor, liver, adipose tissue and COVCAR cells. TP53 mRNA was reverse transcribed and the TP53 cDNA was amplified. We detected a form of the TP53 mRNA transcript with a deletion of nucleotides 115 – 331 corresponding to a loss of 72 amino acids spanning part of the TA domain and the entire proline-rich region. In chickens, Marek's disease virus is known to initiate alternative splicing events of TP53 causing a deletion of the DNA binding domain. *V-src,* a sarcoma-causing virus, is also associated with TP53 deletions. In both cases, deletions in the TP53 mRNA transcript have been demonstrated to occur after exposure to either of the viruses in chicken cancer cell lines. Additionally, the loss of these two domains makes this form of TP53 similar to two human isoforms of TP53 found to be overexpressed in solid tumors. Previous studies

suggest that isoforms lacking the proline-rich region hamper the cell's ability to undergo programmed cell death.

Future Studies

To our knowledge, our study is the first to report this truncated form of TP53 mRNA transcript. Future studies are needed to determine whether the expression of the shortened TP53 mRNA transcript is detected in all tissue types, as well as the extent of full-length TP53 expression. This should be done with White Leghorn hens, other commercial strains, and different species of birds. Furthermore, the genomic TP53 sequence in chickens should be described to determine where alternative splicing events are taking place. An antibody must be made to detect the chicken TP53 protein product expressed in ovarian tumor cells and healthy tissue. Lastly, a study is needed to determine the role of this form of TP53 within the normal TP53 pathway and its relation to tumor development.

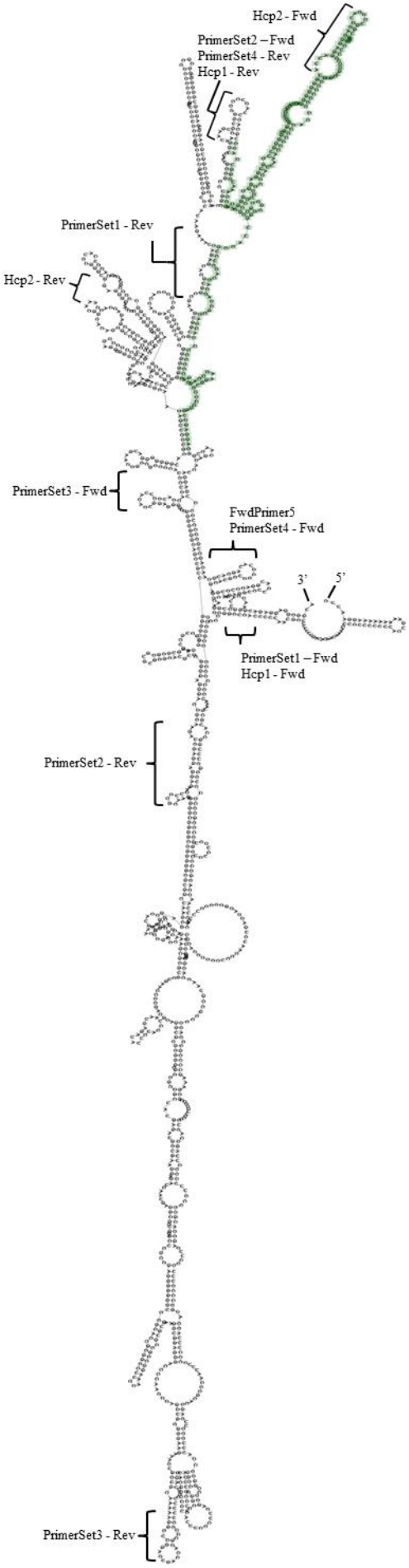
Hcp2 - Fwd
PrimerSet2 – Fwd
PrimerSet4 - Rev
Hcp1 - Rev
PrimerSet1 - Rev
Hcp2 - Rev
PrimerSet3 - Fwd
FwdPrimer5
PrimerSet4 - Fwd
3'
5'
PrimerSet1 – Fwd
Hcp1 - Fwd
PrimerSet2 - Rev
PrimerSet3 - Rev

Figure 5-1. Schematic of the 1153BP TP53 mRNA secondary structure. The secondary structure of the TP53 mRNA transcript forms complex hairpin loops due to the high GC content. The area in which the splicing event occurred contains a high number of GC base pairs. The approximate locations of the primer binding sites are indicated by the labeled brackets. The location of the deletion is highlighted in green. RNA secondary structure prediction was obtained by: Gruber AR, Lorenz R, Bernhart SH, Neuböck R, Hofacker IL. The Vienna RNA Website. Nucleic Acids Res. 2008.

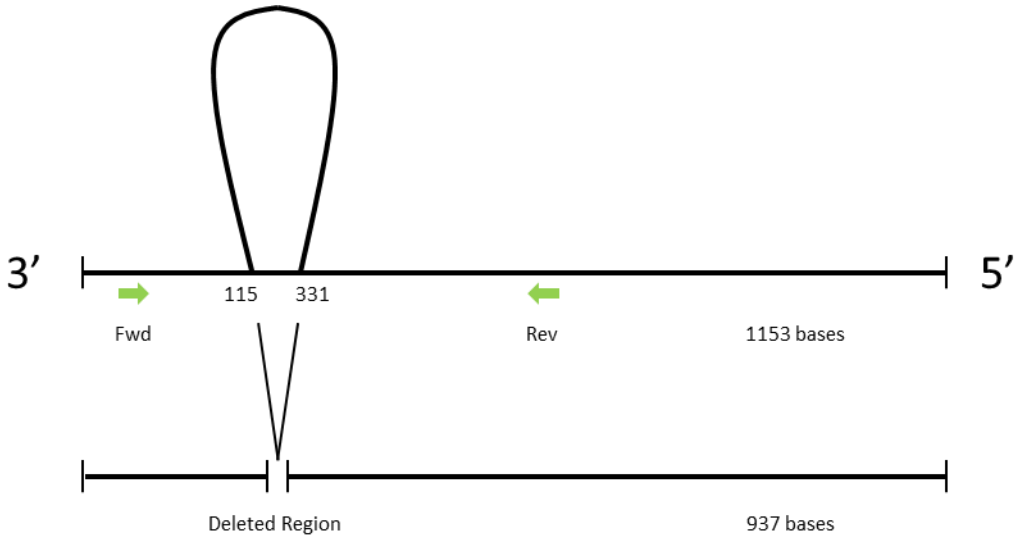

Figure 5-2. Schematic of hairpin loop primer skipping. The secondary structure of the TP53 mRNA transcript forms complex hairpin loops due to the high GC content. Specifically, the area in which our detected splicing event is occurring contains a high number of GC base pairs. The possibility exists for the primer to skip the looped portion of mRNA and continue amplifying, giving the false impression that a deletion exists. Green arrows show the path of the primers. A hairpin loop could be excluded by a primer skipping from the labeled 115 to 331 nucleotides, producing a truncated transcript shown below.

Appendix

Methods Attempted

This section describes PCR methods that were used to attempt to amplify the 3' region of the TP53 mRNA transcript. Total RNA was reverse transcribed according to manufacturer's protocol using PrimeScript reverse transcriptase (Clontech). cDNA was increased from 1 ng to 2 ng in Attempt #2. In Attempt #3, a PCR reaction was performed using 600 nM dNTPs and 600 nM primers of PrimerSet1 and cDNA was increased to 5 ng. The total reaction volume remained at 20 µL. In Attempt #4, a PCR reaction was performed using 300 nM dNTPs and 600 nM PrimerSet1; cDNA (4 ng) was added and reaction volume remained at 20 µL. In Attempt #5, a PCR reaction was performed using the Advantage II GC kit (Clontech) according to the manufacturer's protocol. In Attempt #6, PCR reactions identical to those described in the "methods" section were performed in triplicate and the products pooled for gel extraction. Primers HCP1 and HCP2 were used in PCR reactions as described in the "methods" section in Attempt #7. Finally, a gradient PCR protocol was performed utilizing 55°C, 55.9°C, 56.8°C, and 58°C temperatures in Attempt #8. A summary of the additional attempted PCR reactions is available in Table 6-1.

Table 6-1. Procedures used to amplify the TP53 mRNA transcript.
Summary of changes to the original protocol described in the "methods" section.

Procedure attempted	Changes to original protocol
Attempt 1	RNA reverse transcription via Primescript
Attempt 2	cDNA increased to 2 ng
Attempt 3	dNTP and primer concentration increased to 600 nM
	cDNA increased to 5 ng
Attempt 4	PrimerSet1 concentration inceased to 600 nM
	cDNA increased to 4 ng
Attempt 5	Advantage II GC Polymerase kit used according to manufacturer's protocol
Attempt 6	PCR reactions performed in triplicate
Attempt 7	Primer sets HCP1 and HCP2
Attempt 8	Gradient PCR

References

1 Society, A. C. *Cancer Facts and Figures 2013*, 2013).

2 Vegran, F. *et al.* Only missense mutations affecting the DNA binding domain of p53 influence outcomes in patients with breast carcinoma. *PloS one* **8**, e55103, doi:10.1371/journal.pone.0055103 (2013).

3 Chen, L. M. & Karlan, B. Y. Early detection and risk reduction for familial gynecologic cancers. *Clinical obstetrics and gynecology* **41**, 200-214 (1998).

4 Cannistra, S. A. Cancer of the ovary. *The New England journal of medicine* **351**, 2519-2529, doi:10.1056/NEJMra041842 (2004).

5 Heinonen, P. K., Koivula, T., Rajaniemi, H. & Pystynen, P. Peripheral and ovarian venous concentrations of steroid and gonadotropin hormones in postmenopausal women with epithelial ovarian tumors. *Gynecologic oncology* **25**, 1-10 (1986).

6 Choi, J. H., Choi, K. C., Auersperg, N. & Leung, P. C. Overexpression of follicle-stimulating hormone receptor activates oncogenic pathways in preneoplastic ovarian surface epithelial cells. *The Journal of clinical endocrinology and metabolism* **89**, 5508-5516, doi:10.1210/jc.2004-0044 (2004).

7 Walter F. Boron, E. L. B. *Medical Physiology*. (Elsevier Health Sciences, 2008).

8 Fauci, e. a. Harrison's Principles of Internal Medicine 14th Edition.

9 Kurman, R. J. & Shih Ie, M. The origin and pathogenesis of epithelial ovarian cancer: a proposed unifying theory. *The American journal of surgical pathology* **34**, 433-443, doi:10.1097/PAS.0b013e3181cf3d79 (2010).

10 Scully, R. E. & Richardson, G. S. Luteinization of the stroma of metastatic cancer involving the ovary and its endocrine significance. *Cancer* **14**, 827-840 (1961).

11 Schuler, S., Ponnath, M., Engel, J. & Ortmann, O. Ovarian epithelial tumors and reproductive factors: a systematic review. *Archives of gynecology and obstetrics* **287**, 1187-1204, doi:10.1007/s00404-013-2784-1 (2013).

12 Malpica, A. *et al.* Grading ovarian serous carcinoma using a two-tier system. *The American journal of surgical pathology* **28**, 496-504 (2004).

13 Folkins, A. K. *et al.* Epidemiologic correlates of ovarian cortical inclusion cysts (CICs) support a dual precursor pathway to pelvic epithelial cancer. *Gynecologic oncology* **115**, 108-111, doi:10.1016/j.ygyno.2009.06.032 (2009).

14 Fathalla, M. F. Incessant ovulation--a factor in ovarian neoplasia? *Lancet* **2**, 163 (1971).

15 Murdoch, W. J., Van Kirk, E. A. & Alexander, B. M. DNA damages in ovarian surface epithelial cells of ovulatory hens. *Exp Biol Med (Maywood)* **230**, 429-433 (2005).

16 Casagrande, J. T. *et al.* "Incessant ovulation" and ovarian cancer. *Lancet* **2**, 170-173 (1979).

17 Murdoch, W. J., Murphy, C. J., Van Kirk, E. A. & Shen, Y. Mechanisms and pathobiology of ovulation. *Society of Reproduction and Fertility supplement* **67**, 189-201 (2010).

18 Risch, H. A. Hormonal etiology of epithelial ovarian cancer, with a hypothesis concerning the role of androgens and progesterone. *Journal of the National Cancer Institute* **90**, 1774-1786 (1998).

19 Dubeau, L. The cell of origin of ovarian epithelial tumours. *The Lancet. Oncology* **9**, 1191-1197, doi:10.1016/S1470-2045(08)70308-5 (2008).

20 Medeiros, F. *et al.* The tubal fimbria is a preferred site for early adenocarcinoma in women with familial ovarian cancer syndrome. *The American journal of surgical pathology* **30**, 230-236 (2006).

21 Jacobs, I. J. & Menon, U. Progress and challenges in screening for early detection of ovarian cancer. *Molecular & cellular proteomics : MCP* **3**, 355-366, doi:10.1074/mcp.R400006-MCP200 (2004).

22 Zhang, Z. *et al.* Three biomarkers identified from serum proteomic analysis for the detection of early stage ovarian cancer. *Cancer research* **64**, 5882-5890, doi:10.1158/0008-5472.CAN-04-0746 (2004).

23 Einhorn, N. *et al.* Prospective evaluation of serum CA 125 levels for early detection of ovarian cancer. *Obstetrics and gynecology* **80**, 14-18 (1992).

24 Vanderhyden, B. C., Shaw, T. J. & Ethier, J. F. Animal models of ovarian cancer. *Reproductive biology and endocrinology : RB&E* **1**, 67, doi:10.1186/1477-7827-1-67 (2003).

25 Johnson, P. A. & Giles, J. R. Use of genetic strains of chickens in studies of ovarian cancer. *Poultry science* **85**, 246-250 (2006).

26 Hakim, A. A. *et al.* Ovarian adenocarcinomas in the laying hen and women share similar alterations in p53, ras, and HER-2/neu. *Cancer Prev Res (Phila)* **2**, 114-121, doi:10.1158/1940-6207.CAPR-08-0065 (2009).

27 NCBI. (2014).

28 Leroy, B. *et al.* The TP53 website: an integrative resource centre for the TP53 mutation database and TP53 mutant analysis. *Nucleic acids research* **41**, D962-969, doi:10.1093/nar/gks1033 (2013).

29 Ghebranious, N. & Donehower, L. A. Mouse models in tumor suppression. *Oncogene* **17**, 3385-3400, doi:10.1038/sj.onc.1202573 (1998).

30 Collavin, L., Lunardi, A. & Del Sal, G. p53-family proteins and their regulators: hubs and spokes in tumor suppression. *Cell death and differentiation* **17**, 901-911, doi:10.1038/cdd.2010.35 (2010).

31 Kruse, J. P. & Gu, W. Modes of p53 regulation. *Cell* **137**, 609-622, doi:10.1016/j.cell.2009.04.050 (2009).

32 Chillemi, G. *et al.* Molecular dynamics of the full-length p53 monomer. *Cell Cycle* **12**, 3098-3108, doi:10.4161/cc.26162 (2013).

33 Said, R. *et al.* P53 mutations in advanced cancers: clinical characteristics, outcomes, and correlation between progression-free survival and bevacizumab-containing therapy. *Oncotarget* **4**, 705-714 (2013).

34 Velculescu, V. E. & El-Deiry, W. S. Biological and clinical importance of the p53 tumor suppressor gene. *Clinical chemistry* **42**, 858-868 (1996).

35 Lopez, I. *et al.* Different mutation profiles associated to P53 accumulation in colorectal cancer. *Gene* **499**, 81-87, doi:10.1016/j.gene.2012.02.011 (2012).

36 de Graeff, P. *et al.* Modest effect of p53, EGFR and HER-2/neu on prognosis in epithelial ovarian cancer: a meta-analysis. *British journal of cancer* **101**, 149-159, doi:10.1038/sj.bjc.6605112 (2009).

37 Takagi, M., Ohashi, K., Morimura, T., Sugimoto, C. & Onuma, M. The presence of the p53 transcripts with truncated open reading frames in Marek's disease tumor-derived cell lines. *Leukemia research* **30**, 987-992, doi:10.1016/j.leukres.2005.12.009 (2006).

38 Trtkova, K. & Plachy, J. Deletions in the DNA-binding domain of the TP53 gene in v-src-transformed chicken cells. *In vitro cellular & developmental biology. Animal* **40**, 285-292, doi:10.1290/0312091.1 (2004).

39 Jolly, K. W. *et al.* Splice-site mutation of the p53 gene in a family with hereditary breast-ovarian cancer. *Oncogene* **9**, 97-102 (1994).

40 Surget, S., Khoury, M. P. & Bourdon, J. C. Uncovering the role of p53 splice variants in human malignancy: a clinical perspective. *OncoTargets and therapy* **7**, 57-68, doi:10.2147/OTT.S53876 (2013).

41 Bernard, H. *et al.* The p53 isoform, Delta133p53alpha, stimulates angiogenesis and tumour progression. *Oncogene* **32**, 2150-2160, doi:10.1038/onc.2012.242 (2013).

42 Takagi, M., Ohashi, K., Morimura, T., Sugimoto, C. & Onuma, M. Analysis of tumor suppressor gene p53 in chicken lymphoblastoid tumor cell lines and field tumors. *The Journal of veterinary medical science / the Japanese Society of Veterinary Science* **60**, 923-929 (1998).

43 Mills, A. A. p53: link to the past, bridge to the future. *Genes & development* **19**, 2091-2099, doi:10.1101/gad.1362905 (2005).

44 Soussi, T., Begue, A., Kress, M., Stehelin, D. & May, P. Nucleotide sequence of a cDNA encoding the chicken p53 nuclear oncoprotein. *Nucleic acids research* **16**, 11383 (1988).

45 Schat, K. A., Calnek, B. W., Fabricant, J. & Abplanalp, H. Influence of oncogenicity of Marek' disease virus on evaluation of genetic resistance. *Poultry science* **60**, 2559-2566 (1981).

46 Nigro, J. M. *et al.* Mutations in the p53 gene occur in diverse human tumour types. *Nature* **342**, 705-708, doi:10.1038/342705a0 (1989).

47 Niwa, K. *et al.* Alteration of p53 gene in ovarian carcinoma: clinicopathological correlation and prognostic significance. *British journal of cancer* **70**, 1191-1197 (1994).

48 Lavin, M. F. & Gueven, N. The complexity of p53 stabilization and activation. *Cell death and differentiation* **13**, 941-950, doi:10.1038/sj.cdd.4401925 (2006).

49 Venot, C. *et al.* The requirement for the p53 proline-rich functional domain for mediation of apoptosis is correlated with specific PIG3 gene transactivation and with transcriptional repression. *The EMBO journal* **17**, 4668-4679, doi:10.1093/emboj/17.16.4668 (1998).

50 Toledo, F. *et al.* Mouse mutants reveal that putative protein interaction sites in the p53 proline-rich domain are dispensable for tumor suppression. *Molecular and cellular biology* **27**, 1425-1432, doi:10.1128/MCB.00999-06 (2007).

51 Baptiste, N., Friedlander, P., Chen, X. & Prives, C. The proline-rich domain of p53 is required for cooperation with anti-neoplastic agents to promote apoptosis of tumor cells. *Oncogene* **21**, 9-21, doi:10.1038/sj.onc.1205015 (2002).

52 Berger, M., Vogt Sionov, R., Levine, A. J. & Haupt, Y. A role for the polyproline domain of p53 in its regulation by Mdm2. *The Journal of biological chemistry* **276**, 3785-3790, doi:10.1074/jbc.M008879200 (2001).

53 Campbell, H. G. *et al.* Activation of p53 following ionizing radiation, but not other stressors, is dependent on the proline-rich domain (PRD). *Oncogene* **32**, 827-836, doi:10.1038/onc.2012.102 (2013).

54 Tiwari, A. *et al.* Characterization of ascites-derived ovarian tumor cells from spontaneously occuring tumors of the chicken: evidence for e-cadherin upregulation. *PLoS One (*2013).